https://ntrs.nasa.gov/search.jsp?R=19850024790 2020-03-20T18:16:53+00:00Z

General Disclaimer

One or more of the Following Statements may affect this Document

- This document has been reproduced from the best copy furnished by the organizational source. It is being released in the interest of making available as much information as possible.

- This document may contain data, which exceeds the sheet parameters. It was furnished in this condition by the organizational source and is the best copy available.

- This document may contain tone-on-tone or color graphs, charts and/or pictures, which have been reproduced in black and white.

- This document is paginated as submitted by the original source.

- Portions of this document are not fully legible due to the historical nature of some of the material. However, it is the best reproduction available from the original submission.

Produced by the NASA Center for Aerospace Information (CASI)

DAA (Goddard)

SPACE RADIATION LABORATORY

CALIFORNIA INSTITUTE OF TECHNOLOGY
Pasadena, California 91125

SEMI-ANNUAL STATUS REPORT

for

NATIONAL AERONAUTICS AND SPACE ADMINISTRATION
Grant NGR 05-002-160*
"RESEARCH IN PARTICLES AND FIELDS"

for

1 April 1984 - 31 March 1985

E. C. Stone, Principal Investigator
L. Davis, Jr., Coinvestigator
R. A. Mewaldt, Coinvestigator
T. A. Prince, Coinvestigator

*NASA Technical Officer: Dr. Thomas L. Cline, High Energy Astrophysics

(NASA-CR-176069) RESEARCH IN PARTICLES AND FIELDS Semiannual Status Report, 1 Apr. 1984 - 31 Mar. 1985 (California Inst. of Tech.) 42 p HC A03/MF A01 CSCL 03B

N85-33103

Unclas
G3/93 21909

TABLE OF CONTENTS

TABLE OF CONTENTS

SEMI-ANNUAL STATUS REPORT

NASA Grant NGR 05-002-160

Space Radiation Laboratory (SRL)
California Institute of Technology

1 April 1984 - 31 March 1985

This report covers the research activities in Cosmic Rays, Gamma Rays, and Astrophysical Plasmas supported under NASA Grant NGR 05-002-160. The report is divided into sections which describe the activities, followed by a bibliography.

This group's research program is directed toward the investigation of the astrophysical aspects of cosmic rays and gamma rays and of the radiation and electromagnetic field environment of the Earth and other planets. We carry out these investigations by means of energetic particle and photon detector systems flown on spacecraft and balloons.

1. Cosmic Rays and Astrophysical Plasmas

This research program is directed toward the investigation of galactic, solar, interplanetary, and planetary energetic particles and plasmas. The emphasis is on precision measurements with high resolution in charge, mass, and energy. The main efforts of this group, which are supported partially or fully by this grant, have been directed toward the following two categories of experiments.

1.1. Activities in Support of or in Preparation for Spacecraft Experiments

These activities generally embrace prototypes of experiments on existing or future NASA spacecraft or they complement and/or support such observations.

1.1.1. The High Energy Isotope Spectrometer Telescope (HEIST)

HEIST is a large area (0.25 m^2sr) balloon-borne isotope spectrometer designed to make high-resolution measurements of isotopes in the element range from neon to nickel ($10 \leq Z \leq 28$) at energies of about 2 GeV/nucleon. The instrument consists of a stack of 12 NaI(Tl) scintillators, two Cerenkov counters (C1 and C2), and two plastic scintillators (S1 and S2) as illustrated in Figure 1. Each of the 2-cm thick NaI disks is viewed by six 1.5-inch photomultipliers whose combined outputs measure the energy deposition in that layer. In addition, the six outputs from each disk are compared to determine the position at which incident nuclei traverse each layer to an accuracy of ~2 mm. The Cerenkov counters, which measure particle velocity, are each viewed by twelve 5-inch photomultipliers using light integration boxes. This experiment is a collaborative effort with the Danish Space Research Institute.

ORIGINAL PAGE IS
OF POOR QUALITY

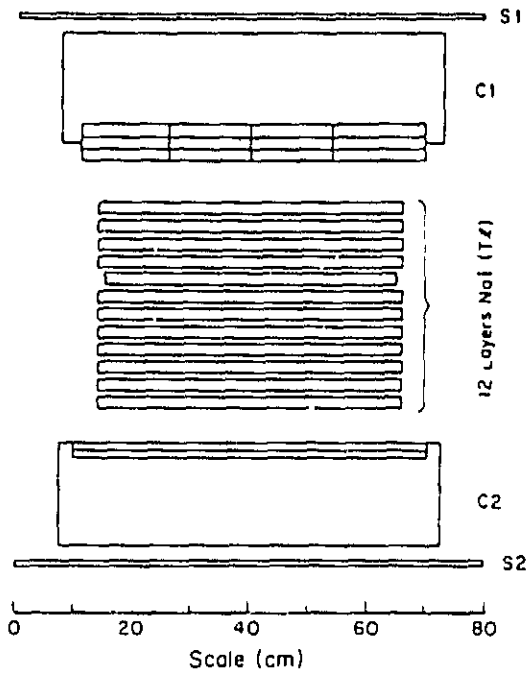

Figure 1

HEIST determines the mass of individual nuclei by measuring both the change in the Lorentz factor ($\Delta\gamma$) that results from traversing the NaI stack, and the energy loss (ΔE) in the stack. Since the total energy of an isotope is given by $E = \gamma M$, the mass M can be determined by $M = \Delta E/\Delta\gamma$. The instrument is designed to achieve a typical mass resolution of 0.2 amu.

On May 14, 1984, the HEIST instrument was launched from Palestine, Texas on its first balloon flight. It reached altitude successfully and floated over Texas for approximately 38 hours at a typical atmospheric depth of ~5.5 g/cm^2, and at geomagnetic cutoffs ranging from ~4.5 to 5.5 GV. During the flight more than 4 x 10^5 events were recorded, including ~10^5 events with charge $Z \geq 6$ and kinetic energy $E \geq 1.4$ GeV/nucleon. Although only a subset of these are suitable for isotope analysis, the others are being used for in-flight mapping and stability checks.

The various HEIST subsystems operated near-perfectly during the flight. Preliminary analysis of the flight data has shown that all of the 108 photomultiplier tubes (PMTs) operated as expected, and that their outputs were stable to $\leq 1\%$ over the course of the flight. The level of stability was a direct result of the successful operation of the automatic evaporative cooling system, which maintained the

internal temperature of the gondola to 25 ± 0.5°C, thereby minimizing the need for temperature-dependent corrections to the gains of the detector electronics, or the NaI light output.

During the past six months significant progress was made in developing algorithms for the determination of the position and energy loss of ions traversing the NaI stack. These algorithms depend on detailed maps of the response of each PMT viewing the NaI; such maps are being derived from the ^{56}Mn Bevalac calibration of HEIST.

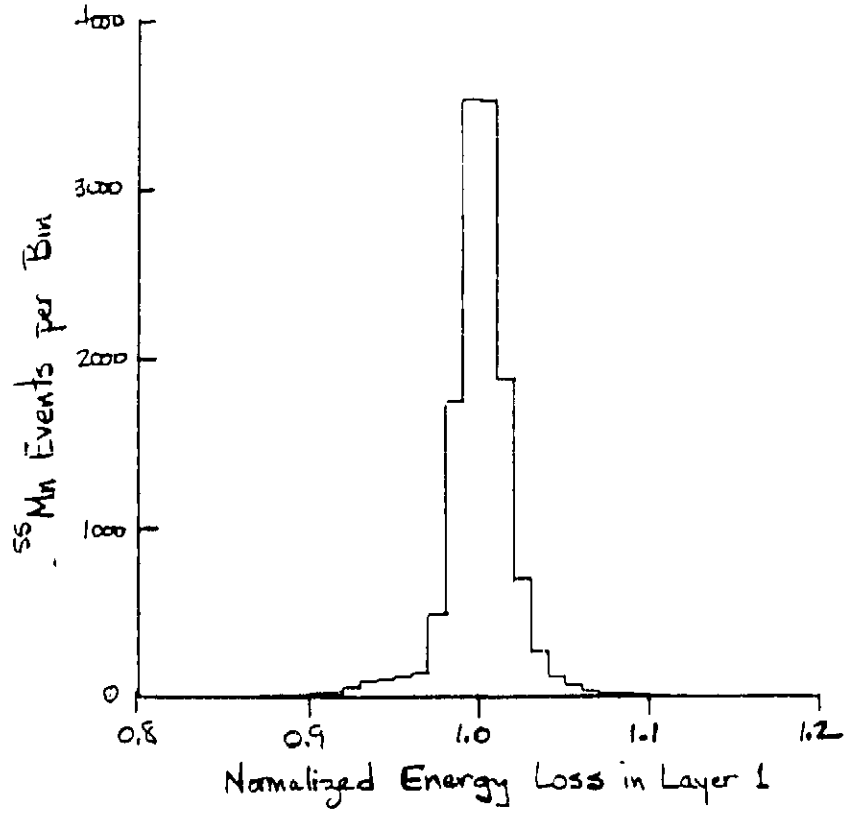

Figure 2

Using these maps in association with appropriate interpolation algorithms we have now achieved an rms energy-loss resolution of ~ 1.2% in the first NaI layer, averaged over the entire area of the disk as shown in Figure 2. This value is only slightly worse than the value achieved (~ 1.0%) in limited regions of the center of the disk. To determine position in the NaI disks we have developed algorithms based on various ratios of the response of the six PMTs viewing each disk. We are now achieving a typical resolution of ~ 2 mm for ^{56}Mn ions incident over ~ 90% of the diameter of the first NaI disk, as illustrated in Figure 3.

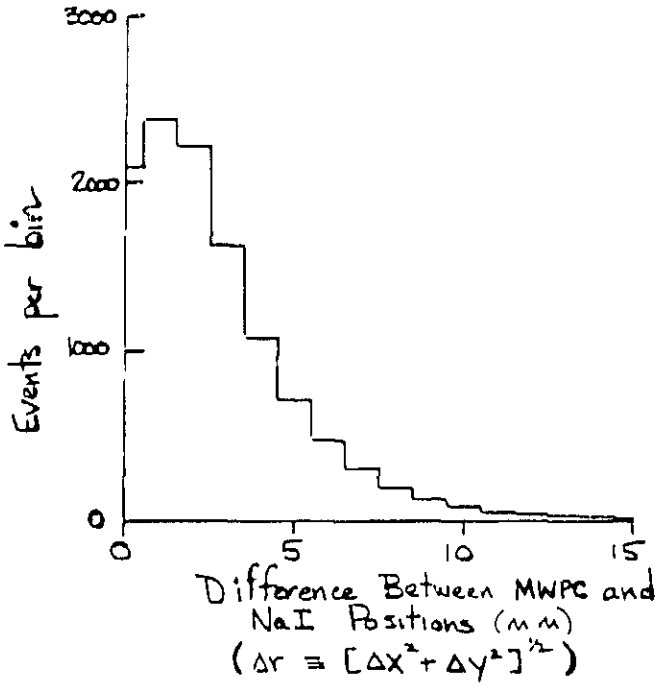

Figure 3

The position and energy resolution currently being achieved is consistent with the requirements for isotope resolution in HEIST. We are now in the process of mapping the NaI layers deeper in the stack so that the information from the various layers can be combined to derive the energy loss of each event, identify nuclear interactions, and determine the trajectory of individual events.

Our colleagues at the Danish Space Research Institute (DSRI) have also received copies of the flight data tapes. They are concentrating their efforts on mapping the response of the two Cerenkov counters, and calibrating the methods for velocity determination.

The following recent talks and papers have resulted from this work:

- "Measurements of Cosmic Ray Isotopes from a Space Station Platform," R. A. Mewaldt, Workshop on Cosmic Rays and High Energy Gamma Ray Experiments for the Space Station Era", Paper presented at the Workshop on Cosmic Rays and High Energy, Louisiana State University, October, 1984 (1984).

- "Initial Results from the Caltech/DSRI Balloon-Borne Isotope Experiment," S. M. Schindler et al., Proc. 19th International Cosmic Ray Conference, La Jolla, California (1985).

A summary of an invited paper that was presented at the LSU Workshop on Space Station Experiments appears below.

MEASUREMENTS OF COSMIC RAY ISOTOPES FROM A SPACE PLATFORM

The isotopic composition of galactic cosmic rays contains a record of the nuclear history of a sample of matter from other regions of the galaxy, including its synthesis in stars, and its subsequent nuclear interactions with the interstellar gas. Although it is only recently that high resolution observations of cosmic ray isotopes became experimentally possible, they have already altered our views of both cosmic ray origin and propagation. In spite of this progress, the rich potential of these studies remains largely unrealized because high-resolution observations to date have been statistically limited - only the most abundant species have so far been measured. Much of the initial progress in this field was made at low energies (~30 to 300 MeV/nucleon) with small solid-state spectrometers carried on spacecraft outside the magnetosphere. Much larger balloon-borne instruments have now been developed to resolve isotopes at energies from ~0.5 to ~2 GeV/nucleon. Recently, consideration has been given to the feasibility of a super-conducting magnet facility for the space station, that, among other objectives, might measure cosmic ray isotopes up to energies as high as ~100 GeV/nucleon. In order to capitalize on these new capabilities and make statistically accurate measurements of rare isotopic species, it will be necessary to expose large instruments outside the atmosphere for periods of a year or more. Such experiments are therefore obvious candidates for a "space platform", either associated with the space station itself, or a "free-flyer" launched into a higher-inclination orbit. In this paper various possibilities for measuring cosmic ray isotopes with $3 \leq Z \leq 30$ from an Earth-orbiting space-platform are considered. It is found that space platform experiments could provide a factor of ~100 improvement in yield over currently approved future experiments. To address the objectives of cosmic ray isotope studies most effectively, measurements should be made by several complementary instruments spanning a range of energies from <0.1 to ~100 GeV/nucleon.

Objectives and Requirements of Cosmic Ray Isotope Studies: Some of the principal objectives of cosmic ray isotope studies include: (1) the study of nucleosynethesis in other regions of the galaxy, (2) measurement of the time-delay between nucleosynthesis and cosmic ray acceleration, and (3) studies of the cosmic ray storage time and pathlength distribution in the galaxy. To address these objectives will require precision measurements of a variety of isotopes with $1 \leq Z \leq 30$, including 1) rare, neutron-rich isotopes of C, O, Ne, Mg, Si, S, Ca, Fe, and Ni; (2) electron-capture isotopes such as ^{57}Co; and (3) radioactive clocks such as ^{10}Be, ^{26}Al, and ^{36}Cl. These measurements must have sufficient mass resolution (≤0.25 amu) and collecting power (e.g., $\geq 10^5$ Si events), preferably in several different energy ranges. For comparison, instruments flown to date have collected a total of fewer than 1000 Si (Z=14) events with $\sigma_m \leq 0.3$ amu. However, the required measurements are now experimentally possible if present-day instruments could be exposed in space for sufficient length of time.

ORIGINAL PAGE IS
OF POOR QUALITY

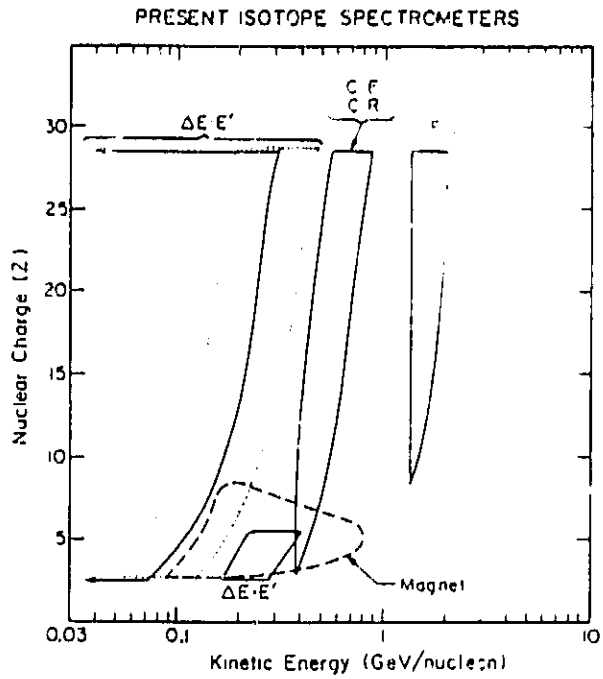

Figure 4

Element and Energy Coverage: Figure 4 summarizes the element and energy ranges covered by representative present-day isotope spectrometers. At the lowest energies the energy loss - total energy ($\Delta E \cdot E'$) technique has been very successful, but is best suited for spacecraft outside the magnetosphere. Except for the magnet experiment, the remaining methods are all based on Cerenkov counters, including the Cerenkov - range ($C \cdot R$), Cerenkov - total energy ($C \cdot E$), and Cerenkov - energy loss - Cerenkov ($C \cdot E \cdot C$) techniques. Note that none of these methods can presently extend above ~2 GeV/nucleon.

ORIGINAL PAGE IS
OF POOR QUALITY

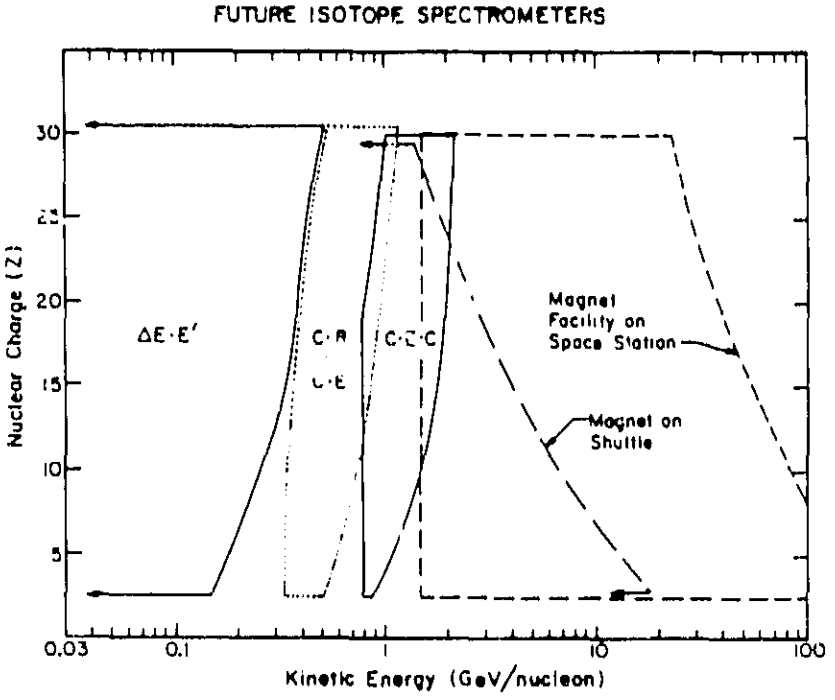

Figure 5

Figure 5 shows estimates of the coverage for future isotope spectrometers. Each of the various Cerenkov techniques can to some extent be "tuned" in energy by selecting the index of refraction of the Cerenkov radiator(s), which allows for some flexibility in the energy and charge ranges covered by a particular instrument (note that a single instrument configuration would not necessarily cover the entire energy range indicated). Also shown in Figure 5 are two possible designs for super-conducting magnet experiments that combine a measurement of the particle's rigidity (provided by the magnet and a trajectory measuring device) with a measurement of the particle's velocity (or momentum/nucleon), perhaps from a Cerenkov counter. The upper limits to the energy range indicated for the "shuttle-compatible" and "space station" versions were determined solely from the assumed rigidity resolution of the magnet; assuming that velocity measuring devices of sufficient accuracy could be developed (undoubtedly a considerable experimental challenge, since to resolve Fe isotopes with σ_m = 0.25 amu requires that the momentum/nucleon be measured to ~0.4 % accuracy or better). It is likely that any given velocity measuring device would function over only a limited portion of the energy range accessible to the magnet. Although a superconducting magnet facility represents a considerably more ambitious undertaking than the "PI-class" experiments in Figures 4 and 5, it offers the possibility of extending cosmic ray isotope measurements into the energy region from ~10 to ~100 GeV/nucleon.

ORIGINAL PAGE IS
OF POOR QUALITY

The Collecting Power of Earth-Orbiting Spectrometers: The principal objective in placing a cosmic ray isotope spectrometer in orbit on a space platform is to improve its yield so that the statistical uncertainty of measurements of rare isotopic species can be minimized. By far the most important gain by a space platform experiment is in the exposure time. None of the existing balloon isotope experiments have been exposed for more than a day or two; this time should be more than a factor of 100 greater on a space platform. The primary disadvantage of an Earth-orbiting platform is the effect of the geomagnetic cutoff.

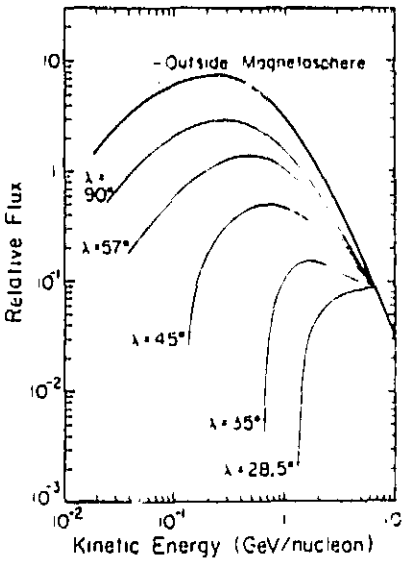

Figure 6

Figure 6 shows the time-averaged spectra that would be observed by an Earth-orbiting cosmic ray experiment for several orbital inclinations. Some of the orbits shown have special significance. The 28.5 deg orbit corresponds to the latitude of Cape Kennedy, and it will undoubtedly be the orbit of the first space station. An orbital inclination of 57 deg is the maximum obtainable with a Cape Kennedy shuttle launch. By launching from Vandenberg AFB on the west coast, a polar orbit (λ = 90 deg) can be obtained. Note that at energies >7 GeV/nucleon the geomagnetic cutoff has no effect. However, using present techniques (including the magnet approach), cosmic ray isotopes are most easily measured at somewhat lower energies, as shown in Figures 4 and 5. In the energy range from ~0.5 to ~2 GeV/nucleon it is clearly important to have a high-inclination orbit ($\lambda \geq 45$ deg), or much of the benefit of the increased exposure time gained by putting an experiment into orbit will be lost.

Yield Estimates: Figure 7 shows how the collecting power of three possible space platform experiments depends on the inclination of the orbit, and also compares these to various (lower-energy) spectrometers on interplanetary-spacecraft that have either flown, or are approved and/or proposed. Note that the C·R, C·E, and C·E·C methods all require a relatively high-inclination orbit to be effective. An advantage of the magnet approach is that it can function at higher energies, and thus is compatible with a 28.5 deg orbit such as the first

space station will have, although in such an orbit it could not contribute measurements below ~2 GeV/nucleon (see Figure 6). Note that each of these three experiments in a suitable orbit (and also an interplanetary Explorer) could easily achieve a factor of ~100 to 1000 increase in yield over experiments that have flown to date (including ISEE-3 and all reported balloon experiments), and they could also improve by a factor of ~100 over presently approved missions such as ISPM (now named Ulysses).

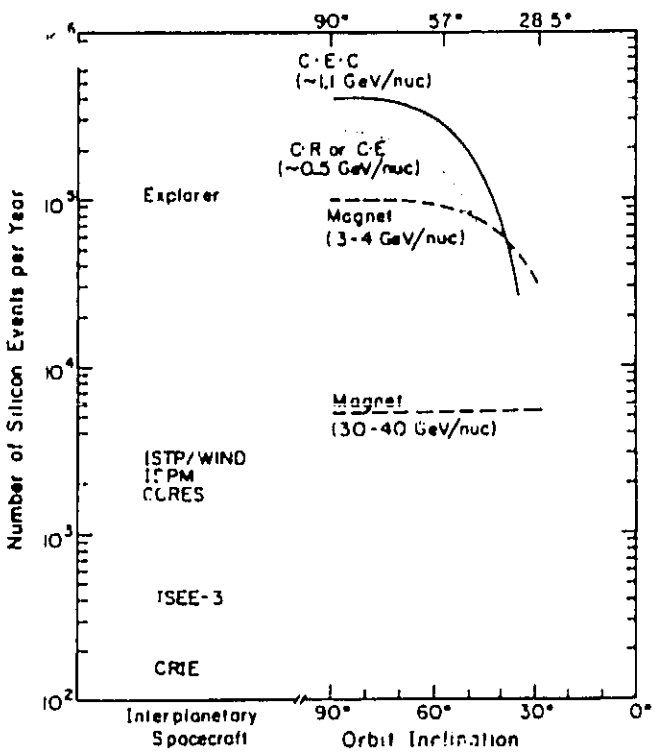

Figure 7

As Figure 7 shows, it is not unreasonable to expect yields of a few times 10^5 Si events per year in several energy ranges if these or similar experiments could be flown in a suitable orbit. Indeed, yields as large as ~10^6 Si per year are possible if the instruments were scaled up further in size over the next few years.

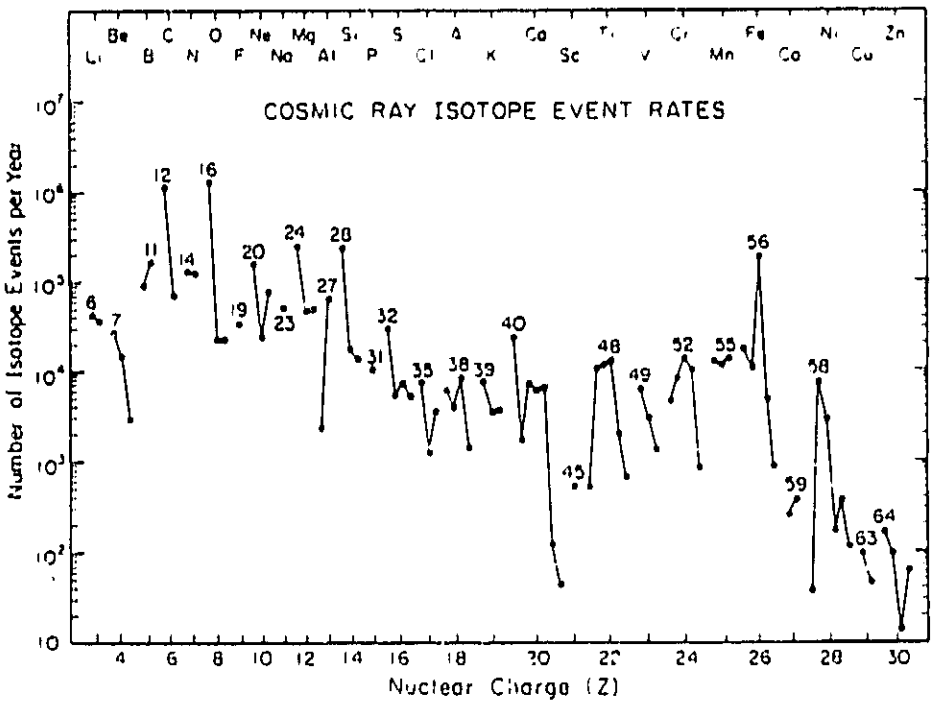

Figure 8

Figure 8 shows the corresponding yield of other isotopes with $3 \leq Z \leq 30$, for $SI \simeq 3 \times 10^5$. Note that for most of the isotopes of interest, including the radioactive clocks, the expected yield ranges from $\sim 10^3$ to $\sim 10^6$ per year, sufficient to make definitive measurements of even rare species.

Summary: In summary, there are now techniques available that can resolve cosmic ray isotopes with $Z \leq 30$ over a wide range in energy, from <0.1 GeV/nucleon up to perhaps even 100 GeV/nucleon. If flown on a space platform such instruments could improve over present or approved experiments by at least two orders of magnitude in yield. In addressing the objectives of cosmic ray isotope studies it will be essential to measure the composition in several different energy ranges. In addition to the time-dilation effects on radioactive clocks, there are other energy-dependent processes, including acceleration by supernova shock waves, fragmentation, solar modulation, and apparently the galactic confinement time, all of which will require broad energy coverage to understand. A super-conducting magnet facility on the space station would make a major contribution to this need by extending isotope measurements to very high energies, thereby making accessible a new range of time-dilation factors for radioactive clocks, and providing a measure of the composition in an energy region where fragmentation corrections are greatly reduced so that the source abundances of a greater number of isotopes could be accurately determined. However, since space station observations will be limited to energies greater than ~2 GeV/nucleon, well above those of the bulk of cosmic ray nuclei, it will be necessary to launch some experiments into higher-inclination orbits and/or outside the magnetosphere if the required energy coverage is to be obtained. For this reason it important that we develop a

number of complementary experimental approaches to measuring cosmic ray isotopes, because it is essential that these studies span as broad an energy range as possible if we are to read accurately the record that cosmic ray isotopes transmit.

1.1.2. Low Energy Isotope Spectroscopy

In August of 1984 we completed a successful calibration of solid-state detectors at the Lawrence Berkeley Laboratory Bevalac, in which we studied several problems important to isotope spectrometers based on silicon solid-state detectors. In particular, we investigated a "charge multiplication" problem that has plagued several thin (~30 to 150 μ) solid-state detectors flown on previous missions. The characteristic of this phenomenon is that the signal from a significant fraction of the particles that lose a great deal of energy in the detector (e.g., stopping Fe ions) is measured to be ~20 to 30% greater than expected, with greatly degraded resolution. At Berkeley we tested a detector from ORTEC that had received special maunufacturing treatments designed to eliminate this problem. Preliminary analysis indicates at least an order of magnitude reduction in the fraction of events exhibiting this problem.

Other areas of investigation during this calibration were an extension of our mass spectroscopy capabilities up to Kr (Z=36) isotopes, further calibrations of position-sensitive solid-state detectors, and further work on determining cosmic ray fragmentation cross sections at low energies. These data are now being analyzed.

1.2. Experiments on NASA Spacecraft

The SR&T grant program of the Space Radiation Laboratory is strengthened by and contributes to the other programs described here. Activities related to these programs are primarily funded by mission-related contracts but grant funds are used to provide a general support base and the facilities which make these programs possible.

1.2.1. An Electron/Isotope Spectrometer (EIS) Launched on IMP-7 on 22 September 1972 and on IMP-8 on 26 October 1973

This experiment is designed to measure the energy spectra of electrons and positrons (0.16 to ~6 MeV), and the differential energy spectra of the nuclear isotopes of hydrogen, helium, lithium, and beryllium (~2 to 50 MeV/nucleon). In addition, it provides measurements of the fluxes of the isotopes of carbon, nitrogen, and oxygen from ~6 to ~15 MeV/nucleon. The measurements from this experiment support studies of the origin, propagation, and solar modulation of galactic cosmic rays; the acceleration and propagation of solar flare and interplanetary particles; and the origin and transport of energetic magnetospheric particles observed in the plasma sheet, adjacent to the magnetopause, and upstream of the bow shock.

The extensive EIS data set has been utilized in comprehensive studies of solar, interplanetary, and magnetospheric processes. Correlative studies have involved data from other IMP investigations and from other spacecraft, as well as direct comparisons of EIS data from IMP-7 and IMP-8. In particular, we are currently using IMP data to support a multidisciplinary workshop that is studying cosmic ray modulation and the large scale structure of the heliosphere.

Our studies of IMP data have resulted in the following recent papers:

- "Microstructure of Magnetic Reconnection in Earth's Magnetotail," J. W. Bieber et al., *J. Geophys. Res.* **89**, 6705 (1984).

- "The Isotopic Composition of the Anomalous Low-Energy Cosmic Rays," R.A. Mewaldt et al., *Ap. J.* **283**, 450 (1984).

- "Solar Cycle Variations of the Anomalous Cosmic Ray Component," R. A. Mewaldt and E. C. Stone, Proc. 19th International Cosmic Ray Conference, La Jolla, California (1985).

- "Cosmic Ray ^{3}He Measurements," R. A Mewaldt, Proc. 19th International Cosmic Ray Conference, La Jolla, California (1985).

1.2.2. An Interstellar Cosmic Ray and Planetary Magnetospheres Experiment for the Voyager Missions Launched in 1977.

This experiment is conducted by this group in collaboration with F. B. McDonald and J. H. Trainor (Goddard Space Flight Center), W. R. Webber (University of New Hampshire), and J. R. Jokipii (University of Arizona), and has been designated the Cosmic Ray Subsystem (CRS) for the Voyager Missions. The experiment is designed to measure the energy spectra, elemental and (for lighter elements) isotopic composition, and streaming patterns of cosmic-ray nuclei from H to Fe over an energy range of 0.5 to 500 MeV/nucleon and the energy spectra of electrons with 3 - 100 MeV. These measurements will be of particular importance to studies of stellar nucleosynthesis, and of the origin, acceleration, and interstellar propagation of cosmic rays. Measurements of the energy spectra and composition of energetic particles trapped in the magnetospheres of the outer planets are used to study their origin and relationship to other physical phenomena and parameters of those planets. Measurements of the intensity and directional characteristics of solar and galactic energetic particles as a function of the heliocentric distance will be used for *in situ* studies of the interplanetary medium and its boundary with the interstellar medium. Measurements of solar energetic particles are crucial to understanding solar composition and solar acceleration processes.

The CRS flight units on both Voyager spacecraft have been operating successfully since the launches on August 20, 1977 and September 5, 1977. The CRS team participated in the Voyager 1 and 2 Jupiter encounter operations in March and July 1979, and in the Voyager 1 and 2 Saturn encounters in November 1980 and August 1981. The Voyager data represent an immense and diverse data base, and a number of scientific problems are under analysis. These investigation topics range from the study of galactic particles to particle

acceleration phenomena in the interplanetary medium, to plasma/field energetic particle interactions, to acceleration processes on the sun, to studies of elemental abundances of solar, planetary, interplanetary, and galactic energetic particles, and to studies of particle/field/satellite interactions in the magnetospheres of Jupiter and Saturn.

The following publications and papers for scientific meetings, based on Voyager data, were generated:

- "Elemental Composition of Solar Energetic Particles," W.R. Cook et al., *Ap. J.* **279**, 827-838 (1984).
- "The Voyager Mission: Encounters with Saturn," E.C. Stone, *J. Geophys. Res.* **88**, 8369 (1983).
- "Voyager Measurements of the Energy Spectrum, Charge Composition, and Long Term Temporal Variations of the Anomalous Components in 1977-1982," W. R. Webber and A. C. Cummings, *Proceedings of Solar Wind V Conference, NASA CP* **2280**, 427-434 (1983).
- "Temporal Variations of the Anomalous Oxygen Component," A. C. Cummings and W. R. Webber, *Proceedings of Solar Wind V Conference, NASA CP* **2280**, 435-440 (1983).
- "The Saturn System," E.C. Stone and T. Owen, *Saturn*, 3 (1984).
- "Evidence that the Anomalous Component is Singly Ionized," A. C. Cummings et al., *Ap. J. (Lett.)* **287**, L99 (1984).

One of these studies is summarized here:

Latitude Variation of Recurrent Protons in the Heliocentric Radial Range 11 to 20 AU and Correlation with Solar Coronal Hole Dynamics.

During the decline to minimum sunspot activity of the last 11-year solar cycle (1973 to 1977) recurring enhancements of MeV-energy nucleon fluxes were found to be closely associated with plasma interaction regions corotating with the sun near the heliographic equator at distances of 1 to 8 AU from the sun. These "corotating interaction regions", or CIRs, develop at the interface between long-lived high speed solar wind streams and lower speed solar wind streams. Recurrent flux enhancements most likely result from the interplanetary acceleration of keV-energy nuclei up to MeV energies by multiple interactions with the hydromagnetic shocks that often form on the leading and trailing edges of the CIRs beyond 1 AU. Elemental composition studies indicate that the keV-energy seed population is most likely the suprathermal tail of the solar wind, although solar flare accelerated nuclei which are also present can be further accelerated along with the interplanetary seed population. Recurrent flux enhancements have previously been used to indicate the presence of the CIRs.

The sources of high speed solar wind streams are now known to be coronal holes, the longest lasting of which cover the poles of the sun during activity minimum. Equatorial extensions of the polar holes are often sources of high speed streams observed near the heliographic equator. Following the peak sun-

spot activity in late 1979 to mid 1980, long-lasting holes reappeared in the sun's corona, allowing investigations of the association between coronal hole and solar wind stream dynamics and the interplanetary acceleration of nuclei to MeV energies to be extended into the outer solar system using data from the Voyager and Pioneer spacecraft.

Spacecraft Observations of Recurrent Phenomena: This study is based on daily samples of the average counting rate of protons in the energy range ~0.5 to 17 MeV from Low Energy Telescopes of the Voyager CRS and the counting rate of ~0.8 to 1.6 MeV protons from the GSFC-UNH Cosmic Ray Experiment aboard the Pioneer 11 spacecraft. Spacecraft distance from the sun (R), latitude (Θ), and longitude (Φ) in an inertial heliographic coordinate system are listed in Table 1 for the start and end of the analysis period. Pioneer 11, midway between the Voyagers in radius, is closer to Voyager 2 in longitude (<7° separation) but is closer to Voyager 1 in latitude (~6° to 9° separation).

Table 1: Trajectory Information

	Voyager 2	Pioneer 11	Voyager 1
R	11.0 - 14.2 AU	13.1 - 16.1 AU	15.1 - 19.8 AU
Θ	2.4°S - 0.8°S	11.7°N - 14.3°N	17.1°N - 23.1°N
Φ	327.1° - 348.4°	329.8° - 342.8°	315.8° - 325.7°

Approximately 450 days of $\geq$ 0.5 MeV-energy proton observations starting in early 1983 appear in Figure 9. To facilitate comparisons, the observation times of spacecraft data have been translated back to the sun assuming a sun-spacecraft propagation delay corresponding to a corotating flow with a constant speed of 500 km/s and are plotted against Carrington Solar Rotation number. An average radial propagation speed of 500 ± 35 km/s was derived using spacecraft radial and longitudinal positions, a solar rotation period of 25.38 days, and measured delay times between correlated recurrent features. Since the spacecraft were close in longitude (<23°), the small additional adjustment for corotation delay was unnecessary in the figure. Features associated with a CIR characterized by 500 km/s line up vertically at the three spacecraft. Recurrent features at Pioneer 11 and Voyager 1 which are associated with a higher speed corotating structure appear to the left of a vertical alignment with Voyager 2, slower characteristic speed structures appear to the right. Similarly, latitude variations of the boundary and width of a solar wind stream's source region cause fluctuations around this vertical organization.

Temporal periodicity is apparent at each spacecraft throughout this time period. This is in direct contrast to observations from Pioneer 10 during the rise to maximum solar activity, when no recurring features were observed beyond 14 AU. During the first twelve solar rotations shown in the figure, the average periods of the recurring proton flux enhancements in the spacecraft reference frames are ~26 days.

Double peaks on a number of recurrent flux enhancements may indicate the presence of either the forward-reverse shock pair on a single CIR or single shocks on two or more merging CIRs.

Three fairly distinct intervals are apparent in Figure 9. During Interval 1, lasting until mid-rotation 1737, the counting rates at all three spacecraft are highly correlated and are dominated by a common 26-day recurrence. The recurrent nature of the proton flux enhancements indicates that CIRs are most likely present, enforcing an ordered structure throughout this region of the

ORIGINAL PAGE IS
OF POOR QUALITY

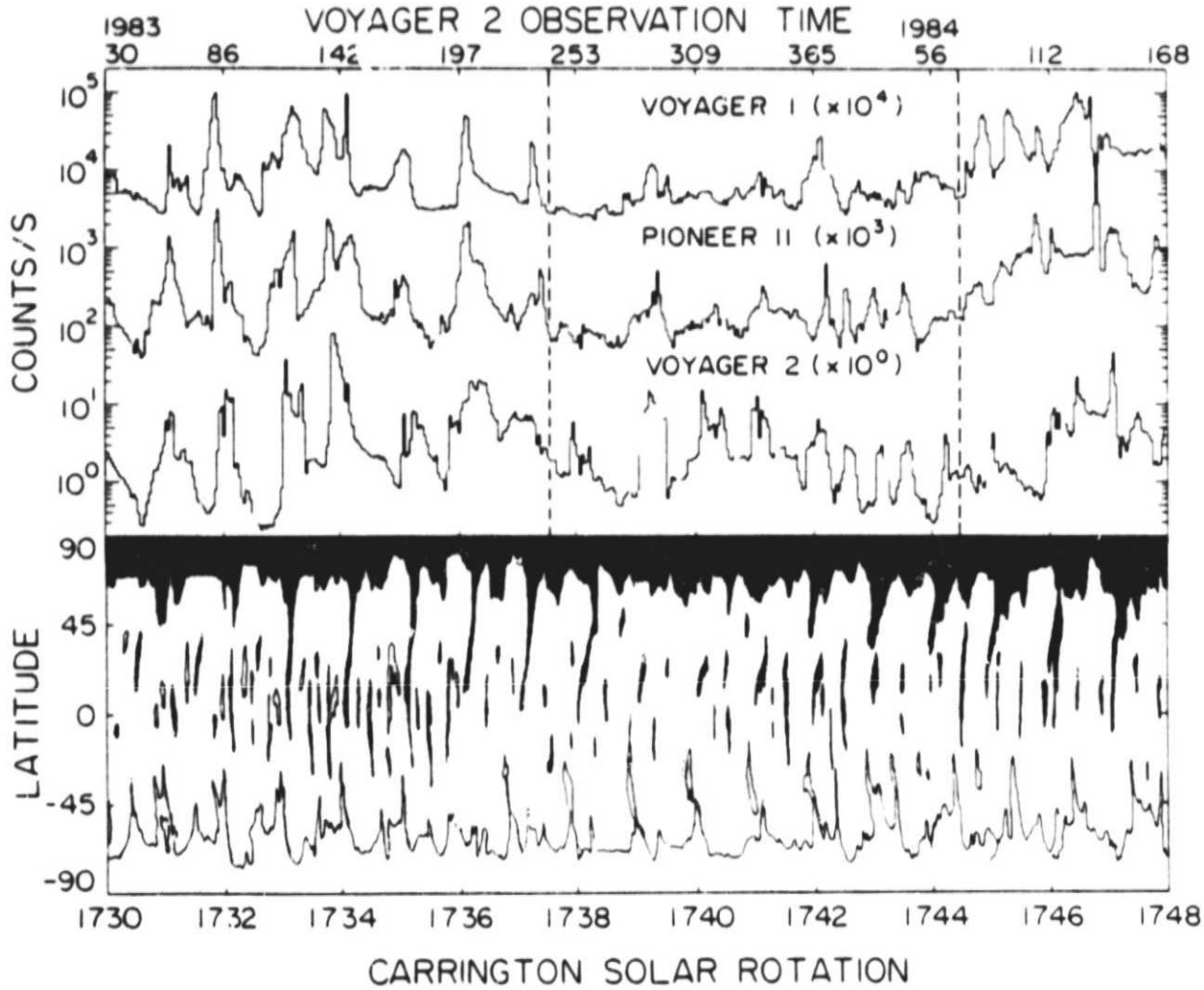

Fig 9: Upper panel: counting rates of ≳ 0.5 MeV-energy protons from the Voyager 1 and 2 and Pioneer 11 spacecraft are plotted versus observation time (Voyager 2 time is indicated) translated back to the sun and identified by Carrington solar rotation number. Dashed lines separate the three analysis intervals discussed in the text.
Lower panel: He 10830 Å coronal hole boundaries are plotted versus Carrington solar rotation number.
heliosphere. The salient point of these observations is the periodicity of the recurrence, not an exact correspondence of the intensity-time profiles.

Interval 2, from mid-rotation 1737 to mid-rotation 1744, is identified by counting rates at all three spacecraft lower than those observed during Interval 1. A common 26-day recurrence is still apparent, although, at times the peaks are barely visible at Voyager 1. On the average, the relative decrease in peak counting rates at Voyager 1 and at Pioneer 11 is approximately twice the relative decrease at Voyager 2. Since Pioneer 11 is closer to Voyager 1 in heliographic latitude but closer to Voyager 2 in distance and longitude, the similari-

ty between Pioneer 11 and Voyager 1 observations indicates that the overall variation in the fluxes is most likely latitudinal, and not radial or temporal in nature.

Interval 3 (after mid-rotation 1744) is characterized by peak flux levels at each spacecraft comparable to those in Interval 1, although now the intensity-time profiles are distinctly different. The interleaving of two 26-day recurrences results in the apparent 13-day periodicity continuing from late in Interval 2 throughout Interval 3. The interleaved 26-day recurrences most probably result from distinct solar sources well separated in heliographic longitude. Strong 13-day recurrences appearing at Voyager 2 and at Pioneer 11 during rotations 1742 and 1743 do not appear at Voyager 1. Thirteen-day peaks during rotations 1744 and 1745 are strongest at Voyager 1, barely discernible at Pioneer 11, and absent at Voyager 2. Since temporal shifts due to radial propagation have already been removed, the staggered appearance of these 13-day series is another indication that distinct latitudinal differences exist and persist into the outer solar system.

Correlations with Coronal Hole Dynamics: Figure 9 also displays estimates of He 10830 Å coronal hole boundaries plotted versus central meridian observation time (identified by Carrington solar rotation number). These inferred coronal hole boundaries and photospheric magnetic polarity information, both derived from earth-based observations, are included in the Hα solar synoptic charts published monthly in *Solar-Geophysical Data Reports*. Coronal holes appearing in regions of dominantly north (south) solar magnetic polarity are shaded (unshaded).

The dominant near equatorial coronal hole during Interval 1 is a long-lived (~7 solar rotations) equatorial extension of the north polar hole. Numerous mid-latitude and equatorial coronal holes, as well as an equatorial extension of the south polar hole, are also visible. Equatorial extensions of polar holes are most often associated with the highest speed solar wind near the heliographic equator, and higher speed streams are known to dominate control of the interplanetary medium. Since two of the spacecraft are north of the equator, the equatorial extension of the north polar coronal hole seems to be the most probable source of the corotating plasma feature controlling the interplanetary medium in the region of the spacecraft. For part of Interval 2 (rotations 1738 to 1744), the north polar extension recedes to well above 45° while two south polar extensions grow, reaching toward the equator, coincident with decreased flux levels at Voyager 1 and Pioneer 11 and with the continuing presence of moderate flux levels at Voyager 2. This suggests that the high speed streams at Voyager 1, at $\lesssim$ 20°N latitude, may emanate from mid-northern latitudes, while those responsible for the continuing moderate flux levels at Voyager 2 may be from a combination of the new equatorial extensions of the south polar hole and the continuing near equatorial holes of northern polarity. Finally, from rotations 1745 to 1747 during Interval 3, the north polar coronal hole re-extends to the equator while, at the same time, the intensities of the recurrent flux enhancements reach levels comparable to those in Interval 1.

The correlated, recurrent enhancements of $\gtrsim$ 0.5 MeV-energy proton flux observed at these three spacecraft for approximately six solar rotations in early 1983 demonstrate that long-lasting structuring of the interplanetary medium by solar wind streams and their CIRs can persist over a latitude range of ~20° out to ~17 AU. Major differences in the intensity of recurrent proton flux enhancements then continue for over ten solar rotations from mid-1983 into

1984, showing that large-scale differences can also exist over a latitude range of only ~20°. Additionally, recurrent proton flux enhancements occurring twice per solar rotation are observed out to at least 19 AU, indicating that CIRs do not necessarily merge within this radius.

These enhancements, which depend upon the dynamics and structure of the heliosphere in the outer solar system, and their apparent correlation with coronal hole dynamics suggest that structuring of the interplanetary medium is still generally controlled by coronal hole dynamics out to ~20 AU and up to 23° latitude from the heliographic equator.

1.2.3. A Heavy Isotope Spectrometer Telescope (HIST) Launched on ISEE-3 in August 1978

HIST is designed to measure the isotope abundances and energy spectra of solar and galactic cosmic rays for all elements from lithium to nickel ($3 \leq Z \leq 28$) over an energy range from several MeV/nucleon to several hundred MeV/nucleon. Such measurements are of importance to the study of the isotopic constitution of solar matter and of cosmic ray sources, the study of nucleosynthesis, questions of solar-system origin, studies of acceleration processes and studies of the life history of cosmic rays in the galaxy.

HIST was successfully launched on ISEE-3 and provided high resolution measurements of solar and galactic cosmic ray isotopes until December 1978, when a component failure reduced its isotope resolution capability. Since that time, the instrument has been operating as an element spectrometer for solar flare and interplanetary particle studies.

Our work on solar flare, interplanetary, and galactic cosmic ray isotopes has resulted in the following recent papers.

- "A High Resolution Study of the Isotopes of Solar Flare Nuclei," R. A. Mewaldt et al., *Ap. J.* **280**, 892 (1984).
- "The Isotopic Composition of the Anomalous Low-Energy Cosmic Rays," R.A. Mewaldt et al., *Ap. J.* **283**, 450 (1984).
- "Measuements of Fe and Ar Fragmentation Cross Sections," K. H. Lau et al., Proc. 19th International Cosmic Ray Conference, La Jolla, California (1985).
- "Solar Cycle Variations of the Anomalous Cosmic Ray Component," R. A. Mewaldt and E. C. Stone, Proc. 19th International Cosmic Ray Conference, La Jolla, California (1985).
- "Cosmic Ray ^{3}He Measurements," R. A. Mewaldt, Proc. 19th International Cosmic Ray Conference, La Jolla, California (1985).

A summary of some of this work appears below.

A New Measurement of the Isotopic Composition of Fe Fragments

One of the natural by-products of calibrating a cosmic ray spectrometer with heavy ion beams is a set of data that can be used to investigate nuclear fragmentation cross-sections of interest to cosmic ray propagation studies.

Our ISEE-3 instrument was calibrated at the Bevalac with beams of ^{56}Fe incident on a CH_2 target at ~ 500 MeV/nucleon. Products of fragmentation reactions in the target were analyzed by HIST as part of the calibration procedure for determining the isotope "tracks" in the various detectors of the instrument. Although the experimental setup did not permit absolute cross-section measurements, it did permit an accurate measurement of the relative yield of the isotopes for a number of elements including Cr, Mn, Fe, and Co. This work constitutes one part of the PhD thesis of K. H. Lau.

An example of the mass distributions obtained for Mn and Fe isotopes is shown in Figure 10. To our knowledge the observed mass resolution of ~ 0.25 amu is the best so far achieved with a cosmic ray instrument for isotopes as heavy as ^{56}Fe. Figure 11 shows the relative yields of Cr, Mn, Fe and Co isotopes that were observed, and compares these observations with the expected yields. The expected yields were calculated using a Monte Carlo calculation based on the semi-empirical cross-section formulae of Tsao and Silberberg. This Monte Carlo approach was developed by Mark Wiedenbeck of the University of Chicago in an earlier collaborative study with us of ^{40}Ar fragmentation. It is hoped that some of the differences that can be seen between the measured and calculated values in Figure 11 will serve as a basis for improvements to the semi-empirical cross-section formulae.

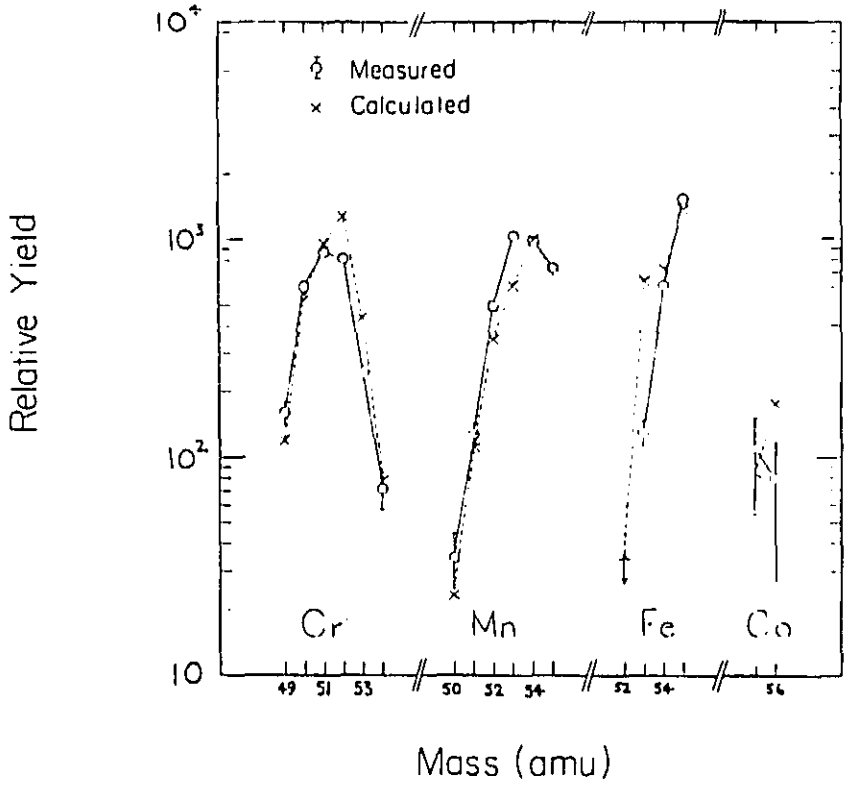

Figure 11

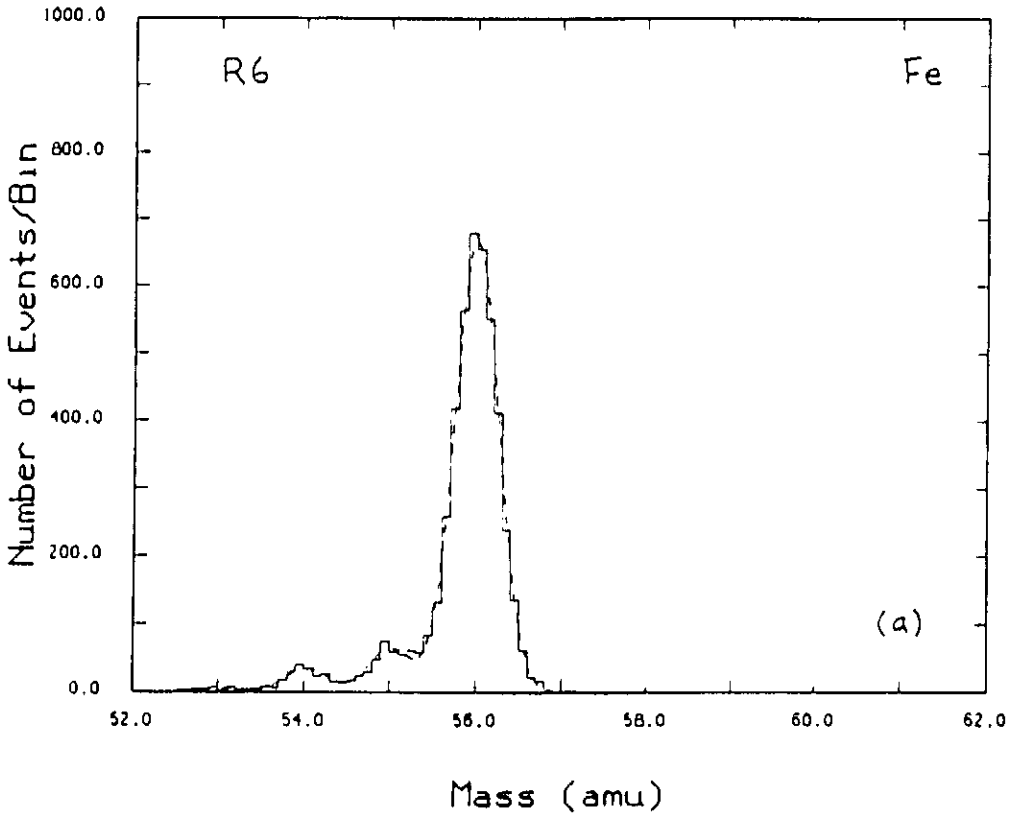
R6
Fe
(a)
Number of Events/Bin
1000.0
800.0
600.0
400.0
200.0
0.0
52.0
54.0
56.0
58.0
60.0
62.0
Mass (amu)

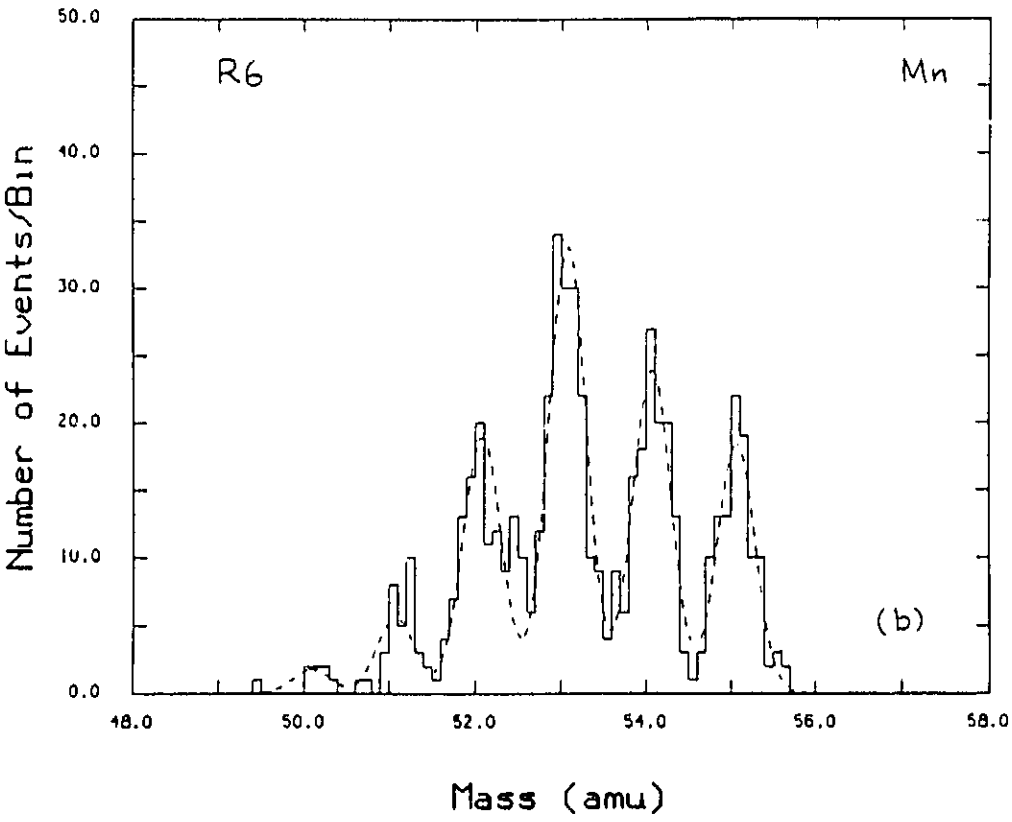
R6
Mn
(b)
Number of Events/Bin
50.0
40.0
30.0
20.0
10.0
0.0
48.0
50.0
52.0
54.0
56.0
58.0
Mass (amu)

Figure 10

1.2.4. A Heavy Nuclei Experiment (HNE) Launched on HEAO-C in September 1979

The Heavy Nuclei Experiment is a joint experiment involving this group and M. H. Israel, J. Klarmann, W. R. Binns (Washington University) and C. J. Waddington (University of Minnesota). HNE is designed to measure the elemental abundances of relativistic high-Z cosmic ray nuclei ($17 \leq Z \leq 130$). The results of such measurements are of significance to the studies of nucleosynthesis and stellar structures, the existence of extreme transuranic nuclei, the origin of cosmic rays, and the physical properties of the interstellar medium. HNE was successfully launched on HEAO-3 and operated until late May 1981.

The following talks and papers were presented during the reporting period:

- "Elemental Abundances of Ultraheavy Cosmic Rays," W.R. Binns et al., *Adv. Space Res.* 4, 25 (1984).

- "HEAO-3 Observations on Nuclei of Platinum and Lead in the Cosmic Radiation," D.J. Fixsen et al., *Bull. of Amer. Phys. Soc.* **29**, 735 (1984).

- "Rigidity Spectra of Ultraheavy Cosmic Ray Results from HEAO-3," M.D. Jones et al., *Bull. Am. Phys. Soc.* **29**, 735 (1984).

- "Elemental Abundances for Cosmic Rays with $26 \leq Z \leq 42$: HEAO-3 Results," W.R. Binns et al., *Bull. Am. Phys. Soc.* **29**, 734 (1984).

The Response of Ionization Chambers to Relativistic Heavy Nuclei

Gas-filled ionization chambers have been used on recent cosmic ray experiments designed to measure heavy element abundances, such as the Heavy Nuclei Experiment (HNE) on HEAO-3 and Ariel VI. The response of such chambers is expected to be proportional to the energy deposited by the particle traversing them. At low energies this energy deposit is simply the ionization energy loss, while at high energies energetic knockon electrons are able to escape from the chamber, reducing the energy deposit.

To first order the ionization energy loss scales as the square of the particle charge Z, however at high Z this assumption breaks down. A more complete expression is given by Ahlen, and predicts an energy loss rising slightly faster than Z^2. Such effects are important when identifying ultraheavy elements.

We have performed two calibrations of ion chambers at the LBL Bevalac using beams ranging from $_{25}$Mn to $_{92}$U. The first, in 1982, was done with a prototype of the HNE ion chamber module which was essentially identical to those used in flight. Thus those data, reported in the 18th ICRC, are directly applicable to our flight experience at the energies calibrated. The second calibration, in 1984, used lab chambers which were made of thinner and more uniform materials, permitting better resolution and better knowledge of the beam energy in each ion chamber, at the cost of less direct relevance to the flight data. Figure 12 is a schematic drawing of the 1984 detector.

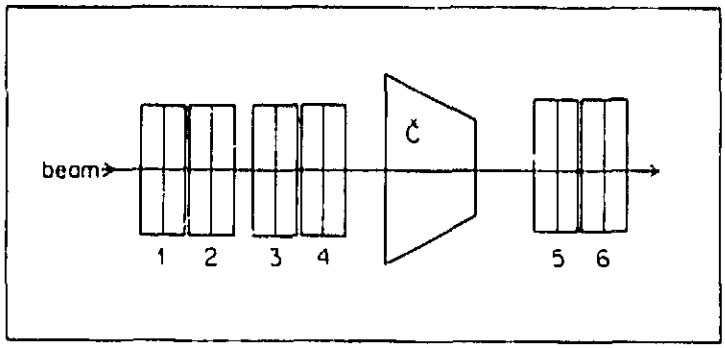

Figure 12

Particles entering the 1984 detector traversed ~0.1 gcm^{-2} of sheet material in the upstream window, rather than the ~1 gcm^{-2} of aluminum honeycomb in the flight prototype; thus the energy loss in the window is much smaller and more uniform. Also, in the 1984 calibration the beam energy was measured with a magnetic spectrometer after being degraded to the calibration energy, rather than being calculated from an energy loss model.

The lab ion chambers had aluminized mylar electrodes (0.8 $mgcm^{-2}$) rather than aluminum screenwire (10 mil diameter, 62.5 mil spacing); thus the production of knockons is much more uniform. A Monte Carlo model of knockon production correctly predicts the degradation in resolution caused by non-uniform production of knockons in the screen wire electrodes. This resolution degradation in the flight chambers tends to mask the relatively subtle deviations from Z^2 scaling.

In 1982 the ultraheavy capabilities of the Bevalac were new and we calibrated only on beams of ~1700 MeV/amu $_{25}$Mn and ~1000 MeV/amu $_{79}$Au. In 1984 beams of $_{26}$Fe, $_{36}$Kr, $_{54}$Xe, $_{67}$Ho, $_{79}$Au, and $_{92}$U nuclei were available at maximum energies of 1666 MeV/amu for Fe to ~839 MeV/amu for U.

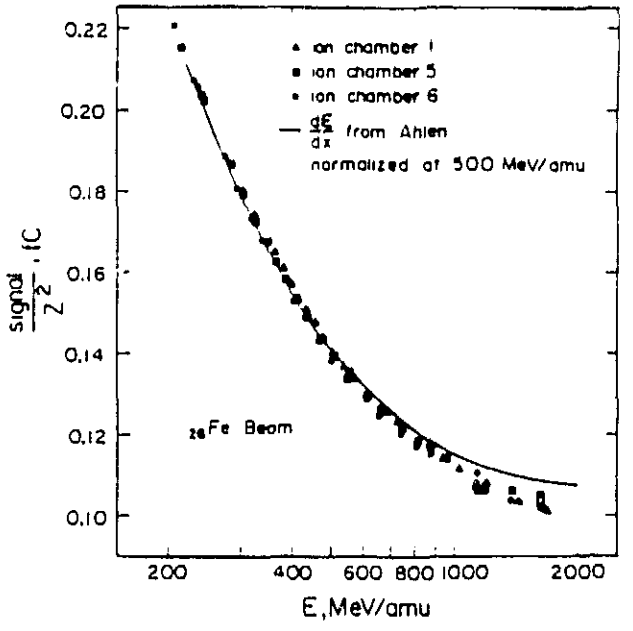

Figure 13

Results of the 1984 Calibration. Figure 13 shows the response of chambers 1,5, and 6 to $_{26}$Fe nuclei as a function of the energy at the midplane of the appropriate chamber, and compares their signals to the calculated dE/dx, arbitrarily normalized at 500 MeV/amu. This normalization corresponds to 27.9 eV per ion pair at low energies for the P-10 gas used (90% argon, 10% methane).

It is apparent that the signals fall below that predicted by dE/dx at energies above 700 MeV/amu. This is somewhat surprising since at these energies we would expect knockons escaping from the exit window to be in equilibrium with those arriving from above, particularly for chambers 5 and 6 which have ~2 gcm^{-2} of upstream material. However, we note that a knockon of a particular energy will be scattered closer to 90° from the incident particle direction as the incident energy increases, and that for energetic knockons the scattering length in a gas may be several cm. Thus the decrease in observed signal may be partly due to knockons escaping from the sides of the chambers.

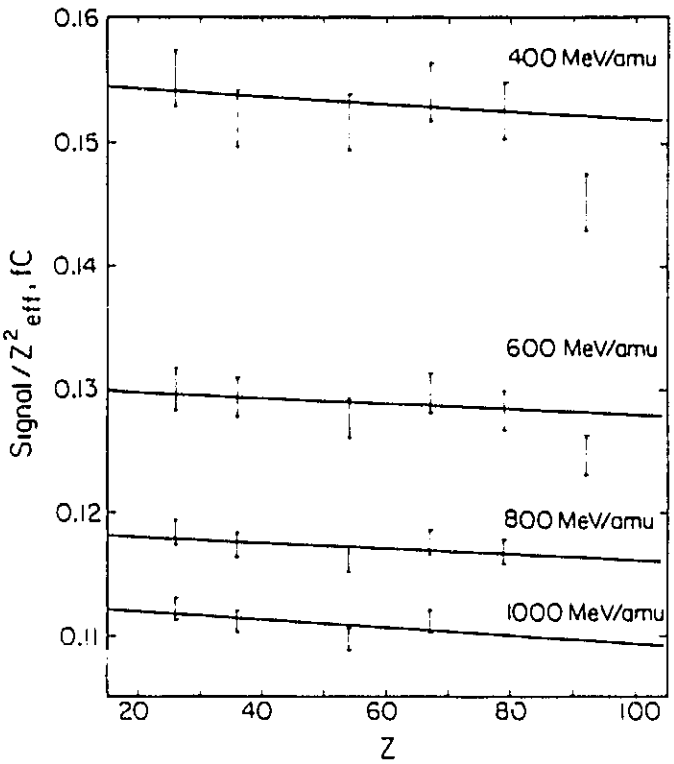

Figure 14

By interpolating to a particular energy we can construct a plot of signal versus Z at that energy. At low energies, the heaviest nuclei have an effective charge, $Z_{eff} = Z[1-\exp(-130\beta Z^{-2/3})]$, due to electron capture. Figure 14 shows the pulse heights, scaled down by Z^2_{eff}, at four energies for Z = 26-92, using ion chambers 1,5, and 8. The straight lines represent a linear fit to the data excluding U, and it is apparent that there is a small negative non-Z^2 effect. The charge of an $_{82}$Pb nucleus would be underestimated by about 0.6 charge units at these energies, in contrast with the charge overestimate of +3 charge units observed for the flight chambers.

Although the non-Z^2 effects in these chambers differ from those observed in the prototype flight chambers, the assumption of Z^2 scaling is still not seriously in error. We also note that our published abundances above charge 50 have used the Čerenkov detector alone to assign charges, and are unaffected by small non-Z^2 effects in the ion chambers.

Since the two calibrations differ, the ionization response to energy loss must be sensitive to details of the mass distribution above, below, and within the chambers. As a result we are using the flight data to directly determine both the energy dependence and effective non-Z^2 correction.

1.2.5. Models of Saturn's Magnetic Field

A reanalysis of the Vector Helium Magnetometer data taken by Pioneer 11 during its encounter with Saturn in 1979 has provided a very good axisymmetric model (designated as the $P_{11}84$ model) of the magnetic field within 8 Saturn radii of the planet. The appropriately weighted root mean square average of the difference between the observed and the modeled field is 1.13% for all the data inside 8 Saturn radii and is 0.40% for all data inside 3 Saturn radii, there being no data inside 1.35 Saturn radii. The difference inside 8 Saturn radii is 1.81% if the $P_{11}84$ model is replaced by the Z_3 model of Connerney, Ness, and Acuna, which is based on data taken by Voyagers 1 and 2. The difference is 1.02% if the Z_3 model is used for the Pioneer 11 data inside 3 Saturn radii. Both the $P_{11}84$ and the Z_3 models are good models, but the $P_{11}84$ model is somewhat better.

The $P_{11}84$ model is better than previous models based on the Pioneer 11 data for several reasons. L. R. Doose has recently provided more accurate data on the roll attitude of Pioneer 11 during the Saturn encounter based on a reexamination of the Pioneer 11 Imaging Photopolarimeter data of Gehrels et al. Some of the one minute averages of the Pioneer 11 data had been excluded from previous analyses because of concerns of their reliability but a careful review determined that they were of high reliability and they are now included in the analysis. It was found that the currents in the bow shock, magnetopause, and ring current regions varied during the encounter and hence that the coefficients in the model that specify the field due to these external sources must have different values after the data gap during occultation than they had before.

For the $P_{11}84$ model the internal source coefficients are $g_1^0 = .2114$, $g_2^0 = .0160$, $g_3^0 = .0226$ Gauss for the internal sources; and for external source coefficients $G_1^0 = -7.1$nT while Pioneer 11 was approaching Saturn and was -12.6 nT while it was leaving.

1.2.6. Proposal for an Advanced Composition Explorer (ACE)

This investigation, proposed jointly by this group, and by W. D. Arnett and J. A. Simpson (University of Chicago), L. F. Burlaga (GSFC), R. E. Gold and S. M. Krimigis (APL/JHU), W. C. Feldman (LANL), G. Gloeckler and G. M. Mason (UMd), and J. V. Hollweg (UNH), is for the study of an Advanced Composition Explorer (ACE). This Explorer-class mission would make comprehensive measurements of the elemental and isotopic composition of accelerated nuclei with increased sensitivity of several orders of magnitude, and with improved mass and charge resolution. ACE would observe particles of solar, interplanetary, and galactic origins, spanning the energy range from that of the solar wind (~ 1 keV/nucleon) to galactic cosmic ray energies (several hundred MeV/nucleon). Definitive studies would be made of the abundance of essentially all isotopes from H to Zn ($1 \leq Z \leq 30$), with exploratory isotope studies extending to Zr ($Z=40$), and element studies extending to U ($Z=92$).

ACE would be a coordinated experimental and theoretical effort, designed to investigate a wide range of fundamental problems. In particular, ACE would provide the first extensive tabulation of solar *isotopic* abundances based on direct sampling of solar material and would establish the pattern of *isotopic differences* between galactic cosmic ray and solar system matter. These composition data would be used to investigate basic dynamical processes that include the formation of the solar corona, the acceleration of the solar wind, and the acceleration and propagation of energetic nuclei on the Sun, in interplanetary space, and in cosmic ray sources. They would also be used to study the history of solar system material and of galactic cosmic ray material, and to investigate the differences in their origin and evolution.

The ACE study payload includes four high resolution spectrometers, each designed to provide the ultimate charge and mass resolution in its particular energy range, and each having a collecting power 1 to 3 orders of magnitude greater than previous or planned experiments. Included in the study would be two spectrometers, a Solar Isotope Spectrometer (SIS) and a Cosmic Ray Isotope Spectrometer (CRIS), for which Caltech would play a leading role. These spectrometers would make use of the proven mass-resolution techniques and large-area detectors that were developed and tested by this laboratory over the past decade, partly through the support of this grant.

1.2.7. Galileo Heavy Ion Counter

This experiment, being constructed by this group in collaboration with N. Gehrels at Goddard Space Flight Center, is being added to the Galileo mission as an engineering subsystem. It will monitor penetrating (~ 10 to ~ 200 MeV/nucleon) sulfur, oxygen, and other heavy elements in the Jovian magnetosphere with the sensitivity needed to warn of potential "single-event upsets" (SEU) in the attitude control system computer. (SEUs are state changes induced by ionizing radiation.) Caltech is responsible for management, detector testing, and calibration of the experiment, which is based on repackaging the Voyager CRS prototype unit (the PTM). Although the primary purpose is engineering support, the data will allow us to continue our investigation of spectra of trapped ions in the Jovian magnetosphere and their relation to the Jovian aurora. In addition, during cruise phase and in the outer Jovian magnetosphere, we will use the instrument to measure the elemental

composition of solar flare events and of the anomalous cosmic ray component, beginning in 1986 and continuing through ~ 1991.

2. Gamma Rays

This research program, which has received significant support from Caltech, is directed toward the investigation of galactic, extragalactic, and solar gamma rays with spectrometers of high angular resolution and moderate energy resolution carried on spacecraft and balloons. The main efforts have been directed toward the following two categories of experiments.

2.1. Activities in Support of or in Preparation for Spacecraft Experiments

These activities generally embrace prototypes of experiments on existing or future NASA spacecraft and they complement and/or support such experiments.

2.1.1. A Balloon-Borne Gamma Ray Imaging Payload (GRIP)

The principal focus of the current gamma-ray astronomy effort is the completion of a balloon-borne imaging gamma-ray telescope for galactic and extragalactic astronomy observations. A shielded NaI Anger camera is used in combination with a 2-cm thick, lead, rotating, coded-aperture mask to achieve an imaging capability of 1070 0.6° pixels in a 20° field of view and a localization capability of 3 arc minutes for 10σ sources. This performance represents more than an order of magnitude improvement over previous balloon and satellite instrumentation. The 16" x 2" NaI Anger camera plate will have an energy range of 30 keV to 5 MeV and achieve a continuum sensitivity of 6×10^{-7} photons/ cm^2 s keV at 1 MeV.

Figure 15 shows a drawing of the detector and coded aperture mask systems of the GRIP instrument. The table lists the key parameters of the instrument. Figures 16a and b are photographs of the instrument taken in early April.

ORIGINAL PAGE IS
OF POOR QUALITY

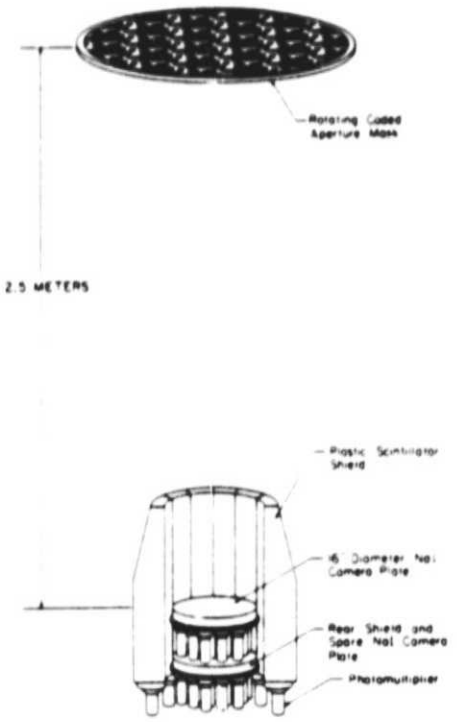

Figure 15

Figure 16a

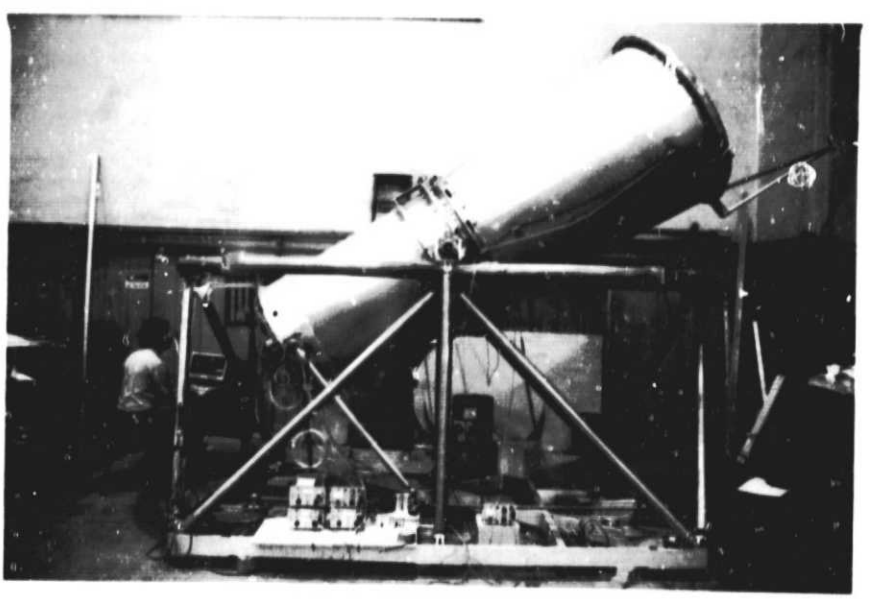

Figure 16b

GRIP Balloon Telescope	
Primary Detector	40 cm x 5 cm NaI Anger Camera Position Resolution: <5 mm FWHM above 100 keV
Shield	Back Plate: 5 cm NaI Side: 16 cm plastic scintillator
Mask	Hexagonal URA: 1.1 m diameter x 2 cm Pb Rotation rate: 1 rpm Spacing: 2.5 m from NaI detector No. of Cells: 1750 (2.5 cm)
Energy Range	0.03 - 5 MeV
Energy Resolution	8.3 keV @ 50 keV; 70 keV @ 1 MeV
Sensitivity (3σ - 8 hr) (Southern Hemisphere)	Continuum: ($\Delta E/E = 1$) @ 100 keV - 1×10^{-5} ph/cm^2 s keV @ 1 MeV - 1×10^{-6} ph/cm^2 s keV Broad Line: ($\Delta E/E$ = 1.2 x FWHM resolution) $\sim 3 \times 10^{-4}$ ph/cm^2 s: 100 keV - 1 MeV
Imaging	Resolution: 1070 0.6° diameter pixels (20° FOV) Angular localization: 3 arc min (10σ source)

Instrument Description

The telescope consists of a shielded detector system separated by 2.5 m from a lead coded-aperture mask. The primary detector is a position-sensitive scintillator which records the characteristic spatial pattern of photons cast by a γ-ray source through the mask.

The mask is made of lead hexagons 2 cm thick and 2.5 cm across (flat-to-flat), supported by an Al honeycomb sandwich which is transparent at γ-ray energies. The aperture contains 2000 hexagonal cells of which half are open and half contain a lead hexagon. The cell pattern (see Figure 17) forms a hexagonal uniformly redundant array (HURA) that is optimal for coded-aperture imaging. HURA's are discussed in more detail in section 2.1.2.

Continuous mask rotation imposes an additional level of coding on the γ-ray signal. Due to the antisymmetry of the coded-aperture pattern under 60 degree rotation (open and closed cells interchange for all but the central cell) the γ-ray signal at each position on the detector is time-modulated with a 50% duty cycle. This feature allows a complete background subtraction to be performed for each detector position once every 20 seconds assuming a 1 rpm rotation rate. In addition, the continuous rotation permits extension of the field of view to 20 degrees, greatly increasing the number of pixels imaged.

The primary detector is a NaI(Tl) camera plate 41 cm in diameter and 5 cm thick. The NaI is viewed by nineteen 3 inch photomultiplier tubes (PMT's) which are individually pulse height analyzed. The PMT gains are calibrated continuously using pulsed LED's for short term relative gain calibration and an ^{241}Am tagged γ-ray source for long term absolute gain calibration. The ^{241}Am source is situated 1 m above the coded-aperture mask and can be imaged continuously during flight, allowing a thorough checkout of the mask-detector imaging system.

ORIGINAL
OF POOR QUALITY

Background suppression is provided by an anti-coincidence shield. On the side are 12 plastic scintillator modules which form a cylinder ~16cm thick. Each module is viewed by a single 5 inch PMT. The lower shield section is a NaI camera plate identical to the primary sensor. Further background suppression is provided by the primary scintillation camera itself. The PMT pulse heights contain information on the depth of the interaction in the crystal. Thus the lower half of the detector can be used as an effective "integral shield" for the reduction of background at low energies.

The telescope is mounted on an elevation pointing platform suspended from an azimuthal torquing system. Azimuthal stabilization and orientation are achieved using active magnetometer feedback to the azimuthal torque motor. Elevation orientation is under command control. Two magnetometers provide 2-axis aspect information accurate to 1.5 arc minutes. This aspect information is recorded in the telemetry stream and allows correction of the event positions for pointing inaccuracies such as displacement and rotation of the telescope field of view.

For the initial flight of GRIP, we will record all nineteen 12 bit PMT pulse heights for each event. Event rates of up to 5×10^3/s are possible and consequently a data recording system with a 1 Mbit/s data rate is required. We have developed a 1.4 Mb/s recording system with 25 Gbyte capacity using commercial VCR's and audio digitizers.

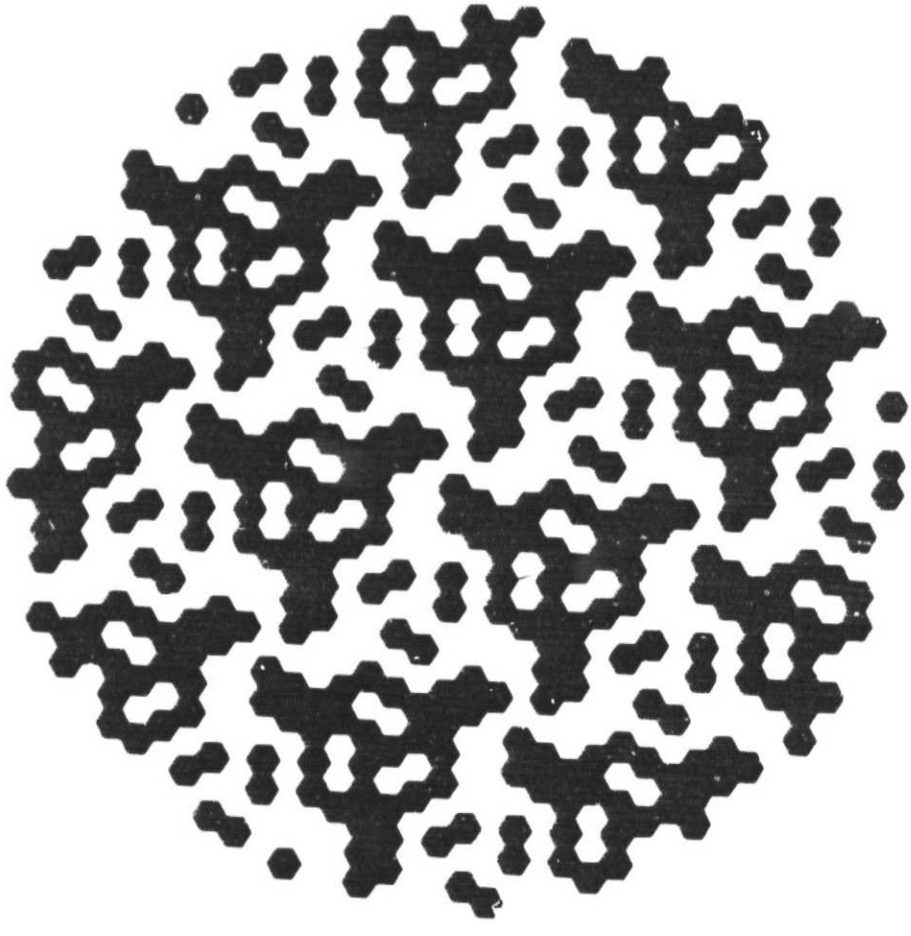

Figure 17

The GRIP scintillation camera has been designed to have ~1 cm FWHM or better position resolution over an energy range from 100 keV to 5 MeV. Figures 18a and 18b show histograms of γ-ray event positions computed by a maximum likelihood method for beams of photons of 122 keV (^{57}Co) and 662 keV (^{137}Cs) incident on the center of the detector. At the lower photon energy, the 10.5 mm FWHM of the distribution is dominated by photon statistics. At the higher photon energy, both Compton scattering and photon statistics contribute to the 7.0 mm width of the distribution. The effect of Compton scattering is most noticeable in the extended non-Gaussian tails of the distribution. The energy resolution of the GRIP scintillation camera is comparable to that of single PMT NaI detectors. We have measured a resolution of 7% FWHM at 662 keV.

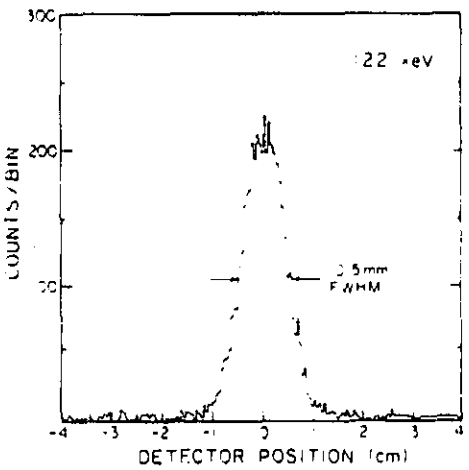

Figure 18a

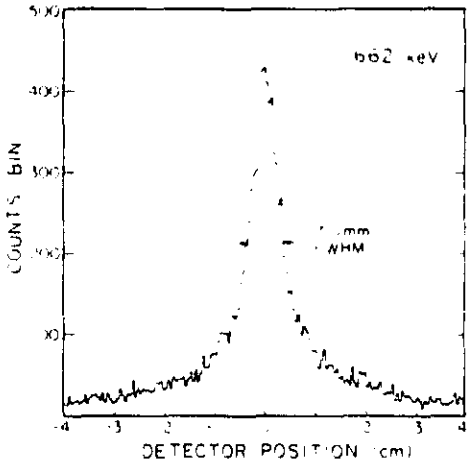

Figure 18b

Figures 19a and 19b are laboratory images of 122 keV and 662 keV γ-ray sources taken with the fully configured GRIP telescope. The sources were suspended 10 m from the coded-aperture mask and the imaging algorithms were adjusted to account for the finite distance to the source. The images demonstrate the ability of the telescope to locate and resolve point sources at γ-ray energies.

ORIGINAL PAGE IS
OF POOR QUALITY

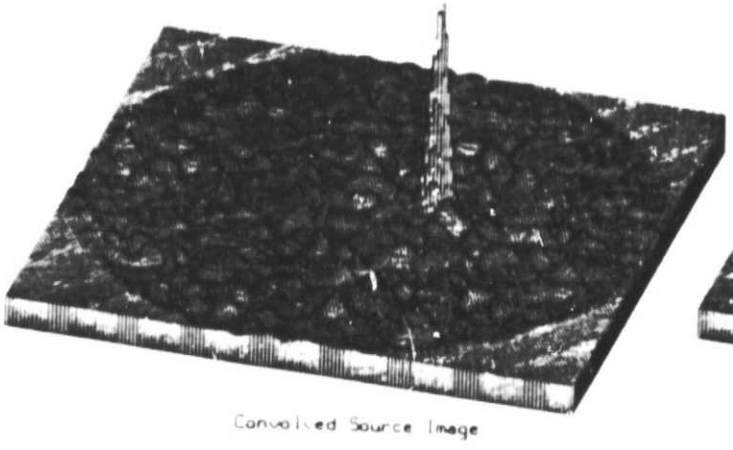

Figure 19a

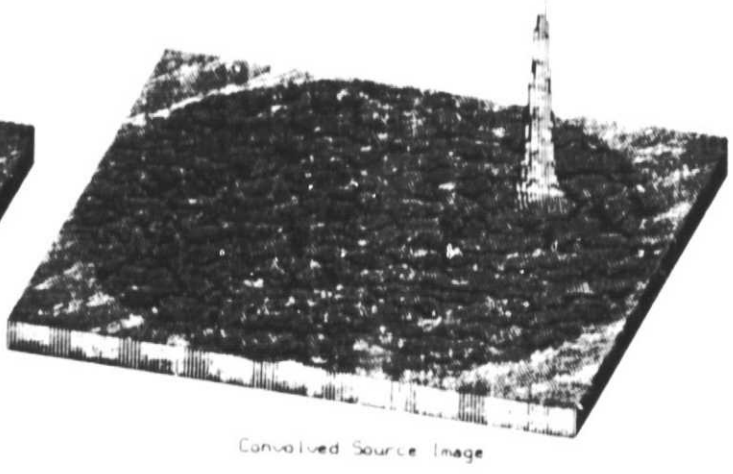

Figure 19b

The instrument technique has been described in:

- "Gamma-Ray Imaging with a Rotating Hexagonal Uniformly Redundant Array," W. R Cook et al., *IEEE Trans. Nuclear Sci.* **NS-31**, 771-775 (1984).

- "A Thick Anger Camera for Gamma-Ray Astronomy," W. R. Cook et al., *IEEE Trans. on Nuclear Science* **NS-31**, 348 (1984).

The GRIP telescope is scheduled for an initial flight from Palestine, Texas in Fall 1985. Observing targets include the Cygnus region, NGC4151, and the Crab region. Future flights are anticipated from both the northern and southern hemispheres. The status of the various instrument subsystems is as follows:

- Telescope: NaI Anger cameras integrated with shield system, telescope enclosure, and flight electronics. High speed VCR recording system taking data at 1.4 Mb/s. Image of laboratory radioactive sources recorded and processed.

- Pointing Systems: (Supported by Caltech Funds) Pointing platform fabricated. Azimuthal torquer fabricated and tested. Elevation motor, ballscrew, and encoder procured and installed.

- Support Systems: Precision magnetometers procured and tested. Precision rotation stage procured and tested. Integration of magnetometers and rotation stage in progress. VCR recording system with 8 VCR units and 25 Gbyte capacity under fabrication. Power system designed and under fabrication. Temperature probe system designed and under fabrication.

We discuss below the coded aperture mask technique used in GRIP.

2.1.2. Hexagonal Uniformly Redundant Arrays for Coded Aperture Imaging

Introduction to URA's. Uniformly redundant arrays are used in coded-aperture imaging, a technique for forming images without mirrors or lenses. This technique is especially important for the high energy x-ray and γ-ray region above 20 keV. In this technique, a mask consisting of opaque (closed) and transparent (open) areas is placed between the photon sources to be imaged and a position sensitive detector or a detector array. Each source casts a shadow pattern of the mask or aperture onto the detector. This shadow pattern may be viewed as an encoded signal for that source direction. If each possible source code is unique, the detected composite of overlapping shadow patterns may be decoded to produce an image of the source distribution.

Figure 17 shows a mask suitable for imaging. This mask consists of an array of open (white) and closed (gray) cells arranged in a periodic pattern. The unit pattern is outlined. The mask in figure 17 is a *uniformly redundant array* (URA). URAs have an especially desirable property: the overlap between two source codes is independent of the source directions as long as the sources are sufficiently separated. Except for periodicity, this guarantees a unique decoding of the composite shadow pattern with a maximal immunity to statistical noise. To date, most work on URAs has concentrated on those constructed on rectangular lattices. Here we focus on URAs constructed on hexagonal lattices, although many of the results are independent of the lattice type.

We have developed procedures for the construction of a special class of URAs, the *skew-Hadamard URAs*, which have the following properties:

1) They are nearly half open and half closed.
2) They are antisymmetric (exchanging open and closed cells) upon rotation by 180° except for the central cell and its repetitions.

Some of the skew-Hadamard URAs constructed on a hexagonal lattice have additional symmetries. These special URAs that have a hexagonal unit pattern, and are antisymmetric upon rotation by 60°, we call *hexagonal uniformly redundant arrays* (HURAs). The mask in figure 17 is an HURA.

HURAs are particularly suited to our application, γ-ray imaging in high background situations. In a high background situation the best sensitivity is obtained with a half open and half closed mask. Furthermore, systematic variations of the detector background from position to position can be larger than the variations in detected flux due to sources. With a skew-Hadamard URA a simple rotation turns the mask into a near anti-mask, allowing exact position-by-position background subtraction. Also, the hexagonal symmetry of an HURA is more appropriate for a round position-sensitive detector or a close-packed array of detectors than a rectangular symmetry. This is especially true for shielded detector systems where compactness is at a premium.

Mathematical Structure of URAs

A URA is defined within a unit pattern which is repeated periodically. The number of cells in this unit pattern is the order v of the URA. Of these cells, k of them are closed and v−k are open. The uniform redundancy property of URAs involves how frequently a given displacement between closed cells occurs. We will consider a cell within a repetition of the unit pattern as equivalent to the corresponding cell in the unit pattern, and will therefore define the difference between two cell centers as the vector displacement between them, folded back into the unit pattern. For a URA, all possible differences occur a

ORIGINAL PAGE IS
OF POOR QUALITY

uniform number λ times among the pairs of closed cell centers. This property guarantees the uniform overlap of source codes discussed in the introduction.

The mathematical structure of a URA is that of an Abelian group difference set, which is specified by an Abelian (additive) group G of order v, and a set D of k elements of G with the property that any possible nonzero difference occurs exactly λ times between elements of D. For a URA the group G is the lattice translations modulo the periods of the mask pattern, and the set D contains those translations that take the central cell to a closed cell. The simplest examples of group difference sets are one-dimensional sets known as *cyclic difference sets* defined on the group of integers mod v. These play an important role in the construction of many URAs. URAs in the class consided here, the *skew-Hadamard URAs*, are nearly antisymmetric. That is, for any nonzero element in the group G, either it or its negative but not both, are contained in the difference set D. These skew-Hadamard URAs are a subset of the *Hadamard URAs* which are nearly half open and half closed. Hadamard URAs are characterized by the parameters $v=4n-1$, $k=2n-1$, $\lambda=n-1$ for some integer n. Two interesting facts about skew-Hadamard URAs have been proven:

1) All skew-Hadamard URAs have a *cyclic* group G, and therefore can be constructed from skew-Hadamard cyclic difference sets.
2) All skew-Hadamard cyclic difference sets are of prime order $v = 3 \bmod 4$ and can be generated from the quadratic residues mod v.

These facts allow us to present a construction for *all* antisymmetric or skew-Hadamard URAs.

Construction of Skew-Hadamard URAs from Quadratic Residues

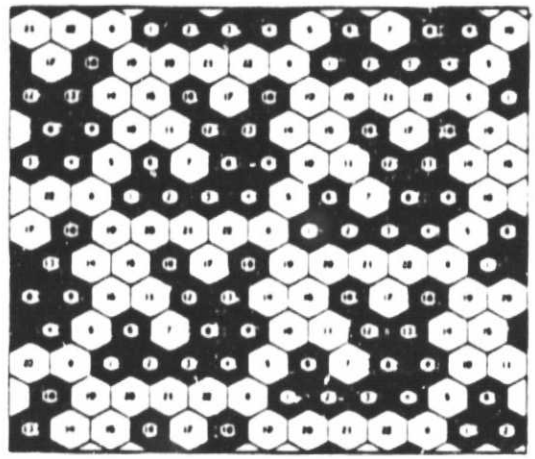

Figure 20

A simple procedure for generating any skew-Hadamard URA has been developed. An example constructed on a hexagonal lattice is shown in figure 20. The procedure consists of the following steps:

1) Choose the lattice on which the URA is to be constructed. The lattice is defined by picking two basis vectors $\vec{e}_0$ and $\vec{e}_1$. For our example we have chosen a hexagonal lattice, which has the basis vectors separated by 60°
2) Choose as the order of the URA a prime of the form $v = 4n-1$. In our example $v = 23$.
3) Construct the order v skew-Hadamard cyclic difference set from the formula

$$D=\{1^2,2^2,\ldots,(\frac{v-1}{2})^2\} \mod v \qquad (1)$$

4) Choose an integer r and label all the cells so that the cell centered at $i\vec{e}_0+j\vec{e}_1$ is labeled with

$$l = (i + rj) \mod v \qquad (2)$$

and make all cells with labels in D closed. In our example r=5.

The heart of this procedure is the construction of the skew-Hadamard cyclic difference set in step 3. Step 4 transfers the difference set properties onto the lattice. This is done through the labeling, which transforms addition mod v to vector addition on the lattice modulo the resulting lattice periods.

The freedom available in this procedure rests in the choice of the lattice, the choice of the order v,and the choice of the multiplier r. The lattice type will determine what symmetries can occur. The possible orders form a rather dense set, the first few choices being v=3,7,11,19,23,31,43,47,59,67,71,79, and 83. The multiplier r determines the periods of the URA, and hence the shape of the unit pattern. Many of the v available choices result in URAs that are related by the symmetries of the lattice.

Hexagonal Uniformly Redundant Arrays

Of the large number of skew-Hadamard URAs, all of which can be constructed by the procedure in the section above, we wish to pick out those that have a hexagonal unit pattern when constructed on a hexagonal lattice. These we call ***hexagonal uniformly redundant arrays*** (HURAs). For an HURA each period when rotated by 60° is again a period. It can be shown from equation (2) that this is only possible if the multiplier r satisfies

$$r^2 = r-1 \mod v \qquad (3)$$

This property has a simple geometric interpretation: a cell labeled l when rotated by 60° will have the label rl mod v. This feature, and the properties of quadratic residues modulo a prime, causes this restricted set of URAs to have a rotational antisymmetry upon rotation by 60° as well as 180°.

In figures 21a thru 21c we show examples of HURAs with orders 139, 151, and 331.

ORIGINAL PAGE IS
OF POOR QUALITY

Figure 21a

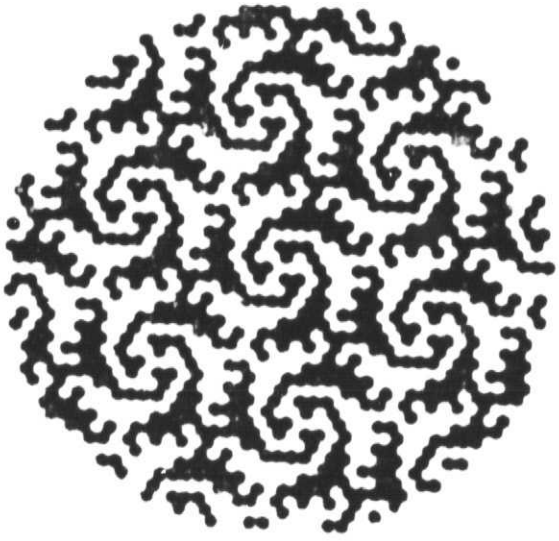

Figure 21b

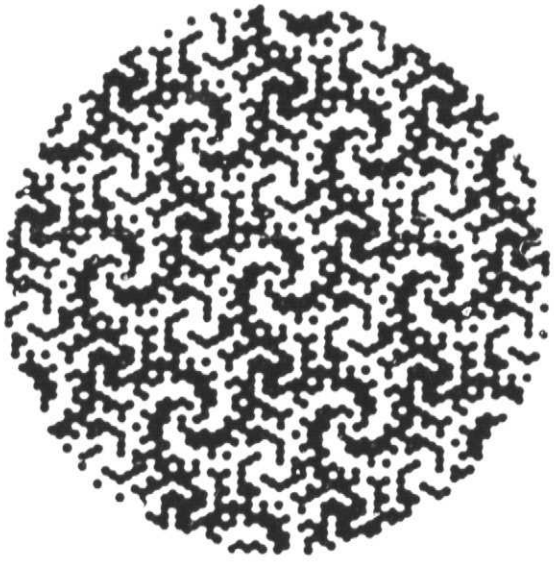

Figure 21c

2.2. Experiments on NASA Spacecraft

The scientific vitality of the SRL gamma ray program is enhanced by collaboration in the analysis of gamma ray data from recent missions. This analysis effort is carried out on the SRL data analysis system.

2.2.1. The Gamma Ray Spectrometer Experiment on the Solar Maximum Mission (SMM)

The Solar Maximum Mission satellite was launched in early 1980 and has been in continuous operation observing gamma-ray emission from solar flares. The University of New Hampshire instrument is sensitive to photons in the energy range 0.3-100 MeV, and can also detect energetic neutrons above 40 MeV.

We have collaborated with U.N.H. in the study of 2.22 MeV emission from neutron capture on hydrogen, following up on our earlier work with the HEAO-3 spacecraft. The focus of the SMM data analysis has been a study of 2.22 MeV line emission in a sample of 8 flares, which includes the very intense solar flare of 3 June 1982. The data from these flares have allowed a detailed study of the time history of the 2.22 MeV neutron capture line from which conclusions have been drawn concerning the production of low energy neutrons in solar flares, the density at which neutrons are captured, and the ^{3}He abundance in the photosphere.

The following invited talk was presented in connection with this work:

- "Gamma-Ray and Neutron Emission from Flares," T. A. Prince, *Bull. Am. Astro. Soc* **16**, 511 (1984).

- "The Energetic Particle and Photon Component of Solar Flares," T.A. Prince, *Bull. Am. Phys. Soc.* **29**, 71 (1984).

2.2.2. Development of a γ-Ray Imager with Arc Second Resolution

A major new activity in the last year has been the definition of an ultra-high-resolution γ-ray imager for solar and cosmic γ-ray astronomy. Above 100 keV, past instruments have been limited to a typical angular resolution of 10° or poorer. The GRIP project described above is a significant step forward with an angular resolution of 0.5° up to energies greater than 1 MeV. It became clear during the last year that an extension of the GRIP technology allows imaging with a resolution of 1 second of arc. A γ-ray imaging device with 1 arc second resolution would be a 10,000 fold improvement over conventional non-imaging instrumentation and have substantial new capabilities for observations of astrophysical gamma-ray sources. With a resolution comparable to that of the VLA and the Einstein X-ray Observatory, the γ-ray imager would make significant contributions to our knowledge of solar flare physics, the galactic center, AGN, and other hard x-ray/γ-ray sources.

The arc second γ-ray imager is based on two previously developed concepts. Fourier transform techniques proposed for x-ray imaging on NASA's

Pinhole/Occulter Facility (P/OF) can be combined with the position sensitive detector development carried out by our group for the GRIP balloon project to achieve greatly improved imaging performance. In essence, pairs of widely separated collimator grids are used to form a large scale modulation pattern of the γ-rays that can be measured by γ-ray detectors with moderate spatial resolution (~1 cm FWHM) such as the GRIP Anger cameras. Each pair of collimator grids measures the phase and amplitude of a particular Fourier component of the source angular distribution. In analogy to radio astronomy, each pair of collimator grids provides one "baseline" for measurement of the angular source distribution.

Planning for the practical implementation of the high-resolution γ-ray imager has taken place within the high-energy solar physics community. This was a natural approach since the concept evolved in part from the P/OF project whose primary objectives are high-resolution studies of the sun. Initial discussions took place in October, 1984 at the Workshop for a High-Energy Facility for Solar Physics. Concurrently, the possibility of an SMM instrument changeout was being discussed for the next solar maximum. High resolution γ-ray imaging is a very attractive option for such a mission. We investigated this possibility in detail and the results were presented at two meetings at the Goddard Space Flight Center in February and April, 1985. The result was a concept for a MAX '91 mission which would include an instrument called GRID (Gamma-Ray Imaging Device). Caltech played a central role in the development of this instrument concept in close cooperation with Marshal Space Flight Center, Goddard Space Flight Center, UCSD, UC Berkeley, and European collaborators from Birmingham, U.K. and Utrecht, Netherlands.

The GRID instrument consists of two collimator grid planes viewed by a complement of x-ray and γ-ray detectors. The collimator grid planes are separated by 6.7 meters. The finest collimator grid scale is 50μ which yields an angular resolution of 1.5 arc seconds. Fabrication of the 1-2 cm thick collimators will be accomplished through stacking of commercially photoetched tungsten grids. For x-ray detectors, xenon-filled multiwire proportional chambers will be used similar to the Birmingham University Spacelab II design. The γ-ray detectors will be similar in design to the Anger cameras developed for the GRIP balloon instrument. The design of the GRID imager is modular with a possibility of accommodating 16-64 collimator pairs.

In the following months, we expect to play a central role in a detailed Phase A study for the MAX '91 mission. Past study activities have received support from this grant as well as from the NSF Presidential Young Investigator Program.

3. Other Activities

R. A. Mewaldt is serving as a member of the High Energy Astrophysics Management Operations Working Group (HEAMOWG), the Cosmic Ray Program Working Group (CRPWG), and as the "OG" program chairman for the 19th International Cosmic Ray Conference.

T. A. Prince has received a Presidential Young Investigator Award from the National Science Foundation.

E. C. Stone continues to serve as NASA's Project Scientist for the Voyager Mission. He is also a member of the Space Science Board, the NASA University

Relations Study Group, and the steering group of the SSB study, "Major Directions for Space Science: 1995-2015"

4. Bibliography

Althouse, W. E. and W. R. Cook, "Balloon-Borne Video Cassette Recorders For Digital Data Storage," Proc. 19th International Cosmic Ray Conference, La Jolla, California (1985).

Althouse, W. E., W. R. Cook, A. C. Cummings, M. H. Finger, T. A. Prince, S. M. Schindler, C. H. Starr, and E. C. Stone, "A Balloon-Borne Gamma-Ray Imaging Telescope," Proc. 19th International Cosmic Ray Conference, La Jolla, California (1985).

Bieber, J. W., E. C. Stone, E. W. Hones, Jr., D. N. Baker, S. J. Bame, and R. P. Lepping, "Microstructure of Magnetic Reconnection in Earth's Magnetotail," *J. Geophys. Res.* **89**, 6705 (1984).

Binns, W.R., D.J. Fixsen, T.L. Garrard, M.H. Israel, J. Klarmann, E.C. Stone, and C.J. Waddington, "Elemental Abundances of Ultraheavy Cosmic Rays," *Adv. Space Res.* **4**, 25 (1984).

Binns, W.R., D.P. Grossman, M.H. Israel, M.D. Jones, J. Klarmann, T.L. Garrard, E.C. Stone, D.J. Fixsen, and C.J. Waddington, "Elemental Abundances for Cosmic Rays with $26 \leq Z \leq 42$: HEAO-3 Results," *Bull. Am. Phys. Soc.* **29**, 734 (1984).

Binns, W. R., N. R. Brewster, D. J. Fixsen, T. L. Garrard, M. H. Israel, J. Klarmann, B. J. Newport, E. C. Stone, and C. J. Waddington, "Lead, Platinum, and Other Heavy Elements in the Primary Cosmic Radiation--HEAO-3 Results," *Ap.J. To be published*, (1985).

Binns, W. R., G. Grimm, M. H. Israel, J. Klarmann, T. L. Garrard, B. J. Newport, and C. J. Waddington, "The Response of Ionization Chambers to Relativistic Heavy Nuclei," Proc. 19th International Cosmic Ray Conference, La Jolla, California (1985)

Binns, W. R., J. Klarmann, M. H. Israel, S. H. Margolis, T. L. Garrard, and C. J. Waddington, "Implications of Observed Source Abundances of Ultraheavy Cosmic Rays," Proc. 19th International Cosmic Ray Conference, La Jolla, California (1985).

Breneman, H.H. and E.C. Stone, "Solar Energetic Particle Abundances of Rare Elements," *Bull. Am. Phys. Soc.* **29**, 706 (1984).

Breneman, H. H. and E. C. Stone, "Precision Measurements of Solar Energetic Particle Elemental Composition," Proc. 19th International Cosmic Ray Conference, La Jolla, California (1985).

Breneman, H. H. and E. C. Stone, "Solar Coronal and Photospheric Abundances from Solar Energetic Particle Measurements," Proc. 19th International Cosmic Ray Conference, La Jolla, California (1985).

Buffington, A., "Calibration of a 12 Inch Astrometric Telescope," *Bull. Am. Phys Soc.* **29**, 685 (1984).

Christon, S. P. and E. C. Stone, "Latitude Variation of Recurrent MeV-Energy Fluxes in the Outer Solar System and Possible Correlation with Solar Coronal Hole Dynamics," *EOS Trans. AGU* **65**, 1034 (Nov, 1984).

Christon, S. P. and E. C. Stone, "Latitude Variation of Recurrent MeV-Energy Proton Flux Enhancements in the Heliocentric Radial Range 11 to 20 AU and Possible Correlation with Solor Coronal Hole Dynamics," *Geophys. Res. Letters* **12**, 109 (1985).

Christon, S. P., A. C. Cummings, and J. X. Zmuidzinas, "The Energy Spectrum of Jovian Electrons Observed in Interplanetary Space," Proc. 19th International Cosmic Ray Conference, La Jolla, California (1985).

Christon, S. P., A. C. Cummings, E. C. Stone, K. W. Behannon, and L. F. Burlaga, "Differential Measurement of Cosmic-Ray Gradient with Respect to Interplanetary Current Sheet," Proc. 19th International Cosmic Ray Conference, La Jolla, California (1985).

Christon, S. P. and E. C. Stone, "Latitude Variation of Recurrent Fluxes in the Outer Solar System," Proc. 19th International Cosmic Ray Conference, La Jolla, California (1985).

Christon, S. P., A. C. Cummings, E. C. Stone, and W. R. Webber, "Solar Modulation and Interplanetary Gradients of the Galactic Electron Flux: 1977-1984," Proc. 19th International Cosmic Ray Conference, La Jolla, California (1985).

Connery, J. E. P., L. Davis, Jr., and D. L. Chenette, "Magnetic Field Models," *Saturn*, Univ.of Arizona Press, 354 (1984).

Cook, W. R, M. Finger, . A. Prince, and E. C. Stone, "Gamma-Ray Imaging with a Rotating Hexagonal Uniformly Redundant Array," *IEEE Trans. Nuclear Sci.* **NS-31**, 771-775 (1984).

Cook, W.R., E.C. Stone, and R.E. Vogt, "Elemental Composition of Solar Energetic Particles," *Ap. J.* **279**, 827-838 (1984).

Cook, W R., M Finger, and T. A. Prince, "A Thick Anger Camera for Gamma-Ray Astronomy," *IEEE Trans. on Nuclear Science* **NS-31**, 348 (1984).

Cummings, A. C. and W. R. Webber, "Temporal Variations of the Anomalous Oxygen Component," *Proceedings of Solar Wind V Conference, NASA CP* **2280**, 435-440 (1983).

Cummings, A. C., E. C. Stone, and W. R. Webber, "Evidence that the Anomalous Component is Singly Ionized," *Ap. J. (Lett.)* **287**, L99 (1984).

Cummings, A. C., E. C. Stone, and W. R. Webber, "Voyager and Pioneer Observations of Anomalous Oxygen During 1983-1984," *EOS Trans. AGU* **65**, 1035 (Nov, 1984).

Cummings, A. C., E. C. Stone, and W. R. Webber, "Changes in the Energy Spectrum of Anomalous Oxygen and Helium During 1977-1985," Proc. 19th International Cosmic Ray Conference, La Jolla, California (1985).

Davis, L. Jr. and E. J. Smith, "Comments on the Paper 'The Z_3 Model of Saturn's Magnetic Field and the Pioneer 11 Vector Helium Magnetometer Observations' by Connery, Acuna, and Ness," *J. Geophys. Res.*, **90**, 4461 (1985).

Finger, M. A. and T. A. Prince, "Hexagonal Uniformly Redundant Arrays for Coded Aperture Imaging," Proc. 19th International Cosmic Ray Conference, La Jolla, California (1985).

Fixsen, D.J., T L. Garrard, M.H. Israel, J. Klarmann, B.J. Newport, E.C. Stone, C.J Waddington, W.R. Binns, and N.R. Brewster, "HEAO-3 Observations on Nuclei of Platinum and Lead in the Cosmic Radiation," *Bull. of Amer Phys. Soc.* **29**, 735 (1984).

Jones, M.D. J. Klarmann, E.C. Stone, C.J. Waddington, W.R. Binns, T.L. Garrard, D.J. Fixsen, and M.H. Israel, "Rigidity Spectra of Ultraheavy Cosmic Ray Results from HEAO-3," *Bull. Am. Phys. Soc.* **29**, 735 (1984).

Jones, M. D., W. R. Binns, M. H. Israel, J. Klarmann, T. L. Garrard, and C. J. Waddington, "Energy Spectra of Iron-Secondary Elements Between 5 and 300 GeV/amu," Proc. 19th International Cosmic Ray Conference, La Jolla, California (1985).

Klarmann, J., W. R. Binns, M. H. Israel, S. H. Margolis, T. L. Garrard, and C. J. Waddington, "Abundances of 'Secondary' Elements Among the Ultraheavy Cosmic Rays-Results from HEAO-3," Proc. 19th International Cosmic Ray Conference, La Jolla, California (1985).

Lau, K. H., R. A. Mewaldt, and E. C. Stone, "Measurements of Fe and Ar Fragmentation Cross Sections," Proc. 19th International Cosmic Ray Conference, La Jolla, California (1985).

Mewaldt, R.A., J.D. Spalding, and E.C. Stone, "The Isotopic Composition of the Anomalous Low-Energy Cosmic Rays," *Ap. J.* **283**, 450 (1984).

Mewaldt, R. A., "Measurements of Cosmic Ray Isotopes from a Space Station Platform," Paper presented at the Workshop on Cosmic Rays and High Energy Gamma Ray Experiments for the Space Station Era, Louisiana State University, October, 1984 (1984).

Mewaldt, R. A., J.D. Spalding, and E.C. Stone, "A High Resolution Study of the Isotopes of Solar Flare Nuclei," *Ap. J.* **280**, 892 (1984).

Mewaldt, R. A. and E. C. Stone, "Solar Cycle Variations of the Anomalous Cosmic Ray Component," Proc. 19th International Cosmic Ray Conference, La Jolla, California (1985).

Mewaldt, R. A., "Cosmic Ray ^{3}He Measurements," Proc. 19th International Cosmic Ray Conference, La Jolla, California (1985).

Newport, B. J., E. C. Stone, C. J. Waddington, W. R. Binns, T. L. Garrard, M. H. Israel, and J. Klarmann, "Elemental Abundances of Cosmic Rays with $Z > 33$ as Measured on HEAO-3," Proc. 19th International Cosmic Ray Conference, La Jolla, California (1985).

Prince, T. A., "Gamma-Ray and Neutron Emission from Flares," *Bull. Am. Astro. Soc.* **16**, 511 (1984).

Prince, T.A., "The Energetic Particle and Photon Component of Solar Flares," *Bull. Am. Phys. Soc.* **29**, 71 (1984).

Schindler, S. M., A. Buffington, E. Christian, E. Grove, K. H. Lau, and E. C. Stone, "Initial Results from the Caltech/DSRI Balloon-Borne Isotope Experiment," Proc. 19th International Cosmic Ray Conference, La Jolla, California (1985).

Stone, E.C., "The Voyager Mission: Encounters with Saturn," *J. Geophys. Res.* **88**, 8389 (1983).

Stone, E.C. and T. Owen, "The Saturn System," *Saturn*, 3 (1984).

Stone, E.C., "Future Studies of Planetary Rings by Spaceprobes," *Planetary Rings*, 687 (1984).

Webber, W. R. and A. C. Cummings, "Voyager Measurements of the Energy Spectrum, Charge Composition, and Long Term Temporal Variations of the Anomalous Components in 1977-1982," *Proceedings of Solar Wind V Conference, NASA CP* **2280**, 427-434 (1983).

Webber, W. R. and A. C. Cummings, "Radial and Latitudinal Gradients of Anomalous Oxygen During 1983-1984," Proc. 19th International Cosmic Ray Conference, La Jolla, California (1985).